

AN *A POSTERIORI* ERROR ANALYSIS FOR THE EQUATIONS OF STATIONARY INCOMPRESSIBLE MAGNETOHYDRODYNAMICS *

JEHANZEB H. CHAUDHRY[†], ARI E. RAPPAPORT[‡], AND JOHN N. SHADID[§]

Abstract. Resistive magnetohydrodynamics (MHD) is a continuum base-level model for conducting fluids (e.g. plasmas and liquid metals) subject to external magnetic fields. The efficient and robust solution of the MHD system poses many challenges due to the strongly nonlinear, non self-adjoint, and highly coupled nature of the physics. In this article, we develop a robust and accurate *a posteriori* error estimate for the numerical solution of the resistive MHD equations based on the exact penalty method. The error estimate also isolates particular contributions to the error in a quantity of interest (QoI) to inform discretization choices to arrive at accurate solutions. The tools required for these estimates involve duality arguments and computable residuals.

Key words. Adjoint-based error estimation, Magnetohydrodynamics, Exact Penalty, finite elements

AMS subject classifications. 65N15, 65N30, 65N50

1. Introduction. The resistive magnetohydrodynamics (MHD) equations provide a continuum model for conducting fluids subject to magnetic fields and are often used to model important applications e.g. higher-density, highly collisional plasmas. In this context, MHD calculations aid physicists in understanding both thermonuclear fusion and astrophysical plasmas as well as understanding the behavior of liquid metals [41, 63]. From a phenomenological perspective, the governing equations of MHD couple Navier-Stokes equations for fluid dynamics with a reduced set of Maxwell's equations for low frequency electromagnetic phenomenon. Structurally, the equations of MHD form a highly coupled, nonlinear, non self-adjoint system of partial differential equations (PDEs). Analytical solutions to the MHD system cannot be obtained for practical configurations; instead numerical solutions are sought. The theoretical and numerical analysis of MHD dates back to the pioneering work of Temam [61]. Finite element formulations of incompressible resistive MHD include stabilization methods based on variational multiscale (VMS) approaches [48, 49, 62], exact and weighted penalty methods [42, 37, 57, 54], first order system least squares (FOSLS) [3, 4, 1, 44] and structure preserving methods [56, 35, 45, 11, 55]. A survey of various numerical techniques for MHD is found in [38]. In this article we restrict ourselves to the

*Submitted to the editors June 5, 2020.

Funding: J. H. Chaudhry's work is supported by the NSF-DMS 1720402. The work of A. E. Rappaport and J. N. Shadid was partially supported by the U.S. Department of Energy, Office of Science, Office of Advanced Scientific Computing Research, Applied Mathematics Program and by the U.S. Department of Energy, Office of Science, Office of Advanced Scientific Computing Research and Office of Fusion Energy Sciences, Scientific Discovery through Advanced Computing (SciDAC) program. Sandia National Laboratories is a multimission laboratory managed and operated by National Technology and Engineering Solutions of Sandia, LLC, a wholly owned subsidiary of Honeywell International, Inc., for the U.S. Department of Energy's National Nuclear Security Administration under contract DE-NA0003525. This paper describes objective technical results and analysis. Any subjective views or opinions that might be expressed in the paper do not necessarily represent the views of the U.S. Department of Energy or the United States Government.

[†]Department of Mathematics and Statistics, University of New Mexico (jehanzeb@unm.edu, <https://math.unm.edu/~jehanzeb>).

[‡]Department of Mathematics and Statistics, University of New Mexico and Center for Computing Research, Sandia National Laboratories, Albuquerque NM (aerappa@sandia.gov).

[§]Center for Computing Research, Sandia National Laboratories, Albuquerque NM and Department of Mathematics and Statistics, University of New Mexico (jnshadi@sandia.gov).

stationary MHD equations based on the exact penalty finite element formulation, originally developed in [42] from a finite element method discretization. We do not employ specialized solver strategies e.g. block preconditioning as the problem size we consider does not merit it.

The numerical solution of complex equations like the MHD equations often have a significant discretization error for solution with significant fine scale spatial structures. This error must be quantified for the reliable use of MHD equations in numerous science and engineering fields. Accurate error estimation is a key component of predictive computational science and uncertainty quantification [29, 30, 17]. Moreover, the error depends on a complex interaction between many contributions. Thus, the availability of an accurate error estimate and the different sources of error also offers the potential of optimizing the choice of discretization parameters in order to achieve desired accuracy in an efficient fashion. In this work we leverage adjoint based *a posteriori* error estimates for a quantity of interest (QoI) related to the solution of the MHD equations. These estimates provide a concrete error analysis of different contributions of error, as well as inform solver and discretization strategies.

In many scientific and engineering applications, the goal of running a simulation is to compute a set of specific QoIs of the solution, for example the drag over a plane wing in the context of the compressible Navier-Stokes equations. Adjoint based analysis [39, 10, 28, 26, 5, 8] for quantifying the error in a numerically computed QoI has found success for a wide variety of numerical methods and discretizations ranging from finite element [16, 29, 33, 21], finite volume [9], time integration [28, 20, 19, 18], operator splitting techniques [29, 33] and uncertainty quantification [31, 32, 17].

Adjoint based *a posteriori* error analysis uses variational analysis and duality to relate errors to computable residuals. In particular, one solves an adjoint problem whose solution provides the residual weighting to produce the error in the QoI. The technique also naturally allows to identify and isolate different components of error arising from different aspects of discretization and solution methods, by analyzing different components of the weighted residual separately.

This article carries out the first adjoint based *a posteriori* error analysis for the MHD equations to the best of our knowledge. The definition of the adjoint operator to the strong form of the MHD system is not obvious since that system is rectangular, and hence the weak form of the exact penalty method is needed for forming the appropriate adjoint problem. We further provide theory supporting the well-posedness of the adjoint weak form. Additionally, the resulting *a posteriori* error estimate is decomposed to identify various sources of error, and the efficacy of the error estimate is demonstrated on a set of benchmark MHD problems.

The remainder of the article is organized as follows. In §2, we review the equations of incompressible resistive MHD, present the exact penalty weak form and the finite element method to numerically solve the problem. In §3 we develop theoretical results for adjoint based *a posteriori* error analysis for an abstract problem representative of the exact penalty weak form. We apply these results to the MHD equations in §4 to develop an *a posteriori* error estimate. In §5 we present numerical results to demonstrate the accuracy and utility of the error estimates produced by our method. In §6 we give details of the derivation of the nonlinear operators in the weak adjoint form as well as a well-posedness argument for the adjoint problem.

2. Exact penalty formulation and discretization. In this section we describe the nondimensionalized equations of incompressible stationary MHD, a stabilized weak form of the MHD system and a finite element method for its solution.

2.1. The MHD equations. Throughout the rest of the paper, let $\Omega \subset \mathbb{R}^d$, $d=2$ or 3 be a bounded, convex polyhedral domain with boundary $\partial\Omega$. The assumptions on the domain are necessary for the solution strategy we choose, as elaborated in §2.3. The nondimensional equations for stationary incompressible MHD in Ω are given by

$$(2.1a) \quad -\frac{1}{\text{Re}}\Delta\mathbf{u} + (\mathbf{u} \cdot \nabla)\mathbf{u} + \nabla p - \kappa(\nabla \times \mathbf{b}) \times \mathbf{b} = \mathbf{f},$$

$$(2.1b) \quad \nabla \cdot \mathbf{u} = 0,$$

$$(2.1c) \quad \frac{\kappa}{\text{Re}_m}\nabla \times (\nabla \times \mathbf{b}) - \kappa\nabla \times (\mathbf{u} \times \mathbf{b}) = \mathbf{0},$$

$$(2.1d) \quad \nabla \cdot \mathbf{b} = 0,$$

where the unknowns are the velocity \mathbf{u} , the magnetic field \mathbf{b} , and the pressure p . The nondimensional parameters are the fluid Reynolds number $\text{Re} > 0$, Magnetic Reynolds number $\text{Re}_m > 0$, and interaction parameter $\kappa = H_a^2/(\text{ReRe}_m)$, where $H_a > 0$ is the Hartmann number. We require the source term $\mathbf{f} \in \mathbf{H}^{-1}(\Omega)$. For $x \in \Omega$ we have $\mathbf{u}(x) \in \mathbb{R}^d$, $\mathbf{b}(x) \in \mathbb{R}^d$, $p(x) \in \mathbb{R}$ and $\mathbf{f}(x) \in \mathbb{R}^d$. We supplement the system (2.1) with boundary conditions,

$$(2.2a) \quad \mathbf{u} = \mathbf{g}, \quad \text{on } \partial\Omega,$$

$$(2.2b) \quad \mathbf{b} \times \mathbf{n} = \mathbf{q} \times \mathbf{n}, \quad \text{on } \partial\Omega.$$

Referring to (2.1), we observe there are $2d + 2$ and only $2d + 1$ unknowns [57]. Effectively enforcing the solenoidal constraint (2.1d) (an involution of the transient MHD system) is an active area of research. Techniques include compatible discretizations [58, 11], vector potential [2, 59] and divergence cleaning [24, 46] as well as the exact penalty method [42, 37, 57]. In this article, we consider the exact penalty method which we further describe in §2.3.

2.2. Function spaces for the MHD system. We make use of the standard spaces $L^2(\Omega)$ and $H^m(\Omega)$ as well as their vector counterparts $\mathbf{L}^2(\Omega)$ and $\mathbf{H}^m(\Omega)$. The $L^2(\Omega)$ (or $\mathbf{L}^2(\Omega)$) inner product is denoted by (\cdot, \cdot) and the norm is denoted by $\|\cdot\|$, while the $H^1(\Omega)$ (or $\mathbf{H}^1(\Omega)$) norm is denoted by $\|\cdot\|_1$. The norm in \mathbb{R}^d is denoted by $\|\cdot\|_{\mathbb{R}^d}$. The details of these function spaces are given in Appendix A. Further useful relations used throughout the text are given in Appendix B and Appendix C. For $\mathbf{b} \in \mathbf{H}^1(\Omega)$, we define $\nabla\mathbf{b} := [\nabla b_1, \dots, \nabla b_d]^T$ as a matrix whose rows are the gradients of the components of \mathbf{b} . The relevant subspaces of $\mathbf{H}^1(\Omega)$ needed to satisfy the boundary conditions (in the sense of the trace operator) are,

$$(2.3) \quad \mathbf{H}_0^1(\Omega) := \{\mathbf{w} \in \mathbf{H}^1(\Omega) : \mathbf{w}|_{\partial\Omega} \equiv \mathbf{0}\},$$

$$(2.4) \quad \mathbf{H}_\tau^1(\Omega) := \{\mathbf{w} \in \mathbf{H}^1(\Omega) : (\mathbf{w} \times \mathbf{n})|_{\partial\Omega} \equiv \mathbf{0}\}.$$

Finally, we define the product space,

$$(2.5) \quad \mathcal{P} := \mathbf{H}_0^1(\Omega) \times \mathbf{H}_\tau^1(\Omega) \times L^2(\Omega).$$

We also remark that for $d = 2$, we use the natural inclusion of $\mathbb{R}^2 \hookrightarrow \mathbb{R}^3$, $[v_1, v_2]^T \mapsto [v_1, v_2, 0]^T$ to define the operators $\nabla \times$ and \times . Thus for $\mathbf{v}, \mathbf{w} \in \mathbf{H}^1(\Omega)$, we have that

$$\nabla \times \mathbf{v} = \left(\frac{\partial v_y}{\partial x} - \frac{\partial v_x}{\partial y} \right) \hat{\mathbf{k}}, \quad \mathbf{v} \times \mathbf{w} = (v_x w_y - v_y w_x) \hat{\mathbf{k}}.$$

2.3. Exact penalty formulation. In this section we present the weak form of the stationary incompressible MHD system based on the exact penalty formulation [42]. The exact penalty method requires that the domain Ω is bounded, convex and polyhedral. This ensures that $\mathbf{H}(\mathbf{curl}, \Omega) \cap \mathbf{H}(\mathbf{div}, \Omega)$ is continuously embedded in $\mathbf{H}^1(\Omega)$ [56, 38]. We also assume homogeneous Dirichlet boundary conditions i.e. $\mathbf{g} = \mathbf{q} = \mathbf{0}$. Non-homogeneous boundary conditions can be dealt with through standard lifting arguments as discussed in §4.3. The exact penalty weak problem corresponding to (2.1) and (2.2) is: find $U = (\mathbf{u}, \mathbf{b}, p) \in \mathcal{P}$ such that

$$(2.6) \quad \mathcal{N}_{EP}(U, V) = (\mathbf{f}, \mathbf{v}), \quad \forall V \in \mathcal{P},$$

where the nonlinear form \mathcal{N}_{EP} is defined for all $V = (\mathbf{v}, \mathbf{c}, q) \in \mathcal{P}$ by

$$(2.7) \quad \begin{aligned} \mathcal{N}_{EP}(U, V) := & \frac{1}{\text{Re}} (\nabla \mathbf{u}, \nabla \mathbf{v}) + (\mathbf{C}(\mathbf{u}), \mathbf{v}) - (p, \nabla \cdot \mathbf{v}) + (q, \nabla \cdot \mathbf{u}) \\ & - \kappa(\mathcal{Y}(\mathbf{b}), \mathbf{v}) - \kappa(\mathcal{Z}(\mathbf{u}, \mathbf{b}), \mathbf{c}) \\ & + \frac{\kappa}{\text{Re}_m} (\nabla \times \mathbf{b}, \nabla \times \mathbf{c}) + \frac{\kappa}{\text{Re}_m} (\nabla \cdot \mathbf{b}, \nabla \cdot \mathbf{c}), \end{aligned}$$

and the nonlinear operators are defined by

$$(2.8a) \quad \mathbf{C}(\mathbf{u}) := (\mathbf{u} \cdot \nabla) \mathbf{u},$$

$$(2.8b) \quad \mathcal{Y}(\mathbf{b}) := (\nabla \times \mathbf{b}) \times \mathbf{b},$$

$$(2.8c) \quad \mathcal{Z}(\mathbf{u}, \mathbf{b}) := \nabla \times (\mathbf{u} \times \mathbf{b}).$$

All except the last term in the weak form arise from multiplying (2.1a)-(2.1c) by test functions and performing integration by parts. The last term, $\frac{\kappa}{\text{Re}_m} (\nabla \cdot \mathbf{b}, \nabla \cdot \mathbf{c})$, effectively enforces the solenoidal involution (2.1d) since, assuming the aforementioned restrictions on the domain, there exists a function (see [42, 40]) $b_0 \in H^2(\Omega)$ such that

$$(2.9) \quad \nabla \cdot \nabla b_0 = \nabla \cdot \mathbf{b}, \quad \text{and} \quad \nabla b_0 \in \mathbf{H}_\tau^1(\Omega).$$

Thus, we choose $V = (\mathbf{0}, \nabla b_0, 0)$ in (2.7) and use (B.1b) so that (2.6) reduces to

$$(2.10) \quad (\nabla \cdot \mathbf{b}, \nabla \cdot \nabla b_0) = (\nabla \cdot \mathbf{b}, \nabla \cdot \mathbf{b}) = 0,$$

and hence (2.1d) is satisfied almost everywhere in Ω .

REMARK 1. The existence of the solution to the problem (2.6) is proven in [42, Theorem 4.6] as well as in [38, Theorem 3.22], while uniqueness is proven in [42, Theorem 4.7] and also in [38, Theorem 3.22]. Both uniqueness proofs rely on a “small data” assumption, i.e. inequalities bounding the nondimensionalised constants, Re, Re_m and κ , in terms of the data \mathbf{f}, \mathbf{g} and \mathbf{q} .

2.4. Finite element method. We introduce the standard continuous Lagrange finite element spaces. Let \mathcal{T}_h be a simplicial decomposition of Ω , where h denotes the maximum diameter of the elements of \mathcal{T}_h , such that the union of the elements of \mathcal{T}_h is Ω , and the intersection of any two elements is either a common edge, node, or is empty. The standard Lagrange space finite element space of order q is then

$$(2.11) \quad \mathbb{P}_h^q := \{v \in C(\Omega) : \forall K \in \mathcal{T}_h, v|_K \in \mathbb{P}^q(K)\},$$

where $\mathbb{P}^q(K)$ is the space of polynomials of degree at most q defined on the element K . Additionally, our finite element space satisfies the Ladyzhenskaya-Babuška-Brezzi

condition stability condition [12] for the velocity pressure pair, e.g. $\mathcal{P}_h = \mathbb{P}_h^2(\Omega) \times \mathbb{P}_h^1(\Omega) \times \mathbb{P}_h^1(\Omega)$. Then the discrete problem to find an approximate solution $U_h = (\mathbf{u}_h, \mathbf{b}_h, p_h) \in \mathcal{P}_h$ to (2.7) is,

$$(2.12) \quad \mathcal{N}_{EP}(U_h, V_h) = (\mathbf{f}, \mathbf{v}_h) \quad \forall V_h \in \mathcal{P}_h.$$

Note there is no restriction on the finite element space for \mathbf{b}_h , which is an advantage of this method. The existence and uniqueness of the solution of the discrete problem (2.12) is also demonstrated in Gunzburger et al. [42] with the same assumptions of the data as discussed in Remark 1.

2.5. Quantity of interest (QoI). The goal of a numerical simulation is often to compute some functional of the solution, that is, the QoI. In particular, QoIs considered in this article have the generic form,

$$(2.13) \quad \text{QoI} = \int_{\Omega} \Psi \cdot U \, dx = (\Psi, U)$$

where U is defined by (2.6) and $\Psi \in \mathbf{L}^2(\Omega) \times \mathbf{L}^2(\Omega) \times L^2(\Omega) \equiv [L^2(\Omega)]^{2d+1}$. For example in two dimensions, to compute the average of the y component of velocity u_y over a region $\Omega_c \subset \Omega$, set $\Psi = \frac{1}{|\Omega_c|} [0, \mathbb{1}_{\Omega_c}, 0, 0, 0]^T$, where $\mathbb{1}_S$ denotes the characteristic function over a set S . In the examples presented later, the QoIs physically represent quantities representative of the average flow rate, or the average induced magnetic field. We seek to compute error estimates in the QoI using duality arguments as presented in the following subsection.

3. Abstract *a posteriori* error analysis. In this section we consider an abstract variational setting for a *a posteriori* analysis based on the ideas from [28, 25, 39, 5, 8]. Let \mathcal{W} be a Hilbert space with inner-product $\langle \cdot, \cdot \rangle$ and let \mathcal{V} be a dense subspace of \mathcal{W} . Throughout this section $u \in \mathcal{V}$ refers to the solution of an abstract variational problem (e.g. solution of (3.3) or (3.8)). An example of such a variational problem is the exact penalty problem as described in §2.3. Moreover, we denote $u_h \in \mathcal{V}_h$ as a numerical approximation to u , where \mathcal{V}_h is a finite dimensional subspace of \mathcal{V} , and denote the error as $e = u - u_h$. Finally, w and v refer to arbitrary functions, and their spaces are made clear when we use these functions. For the QoI, consider bounded linear functionals of the form,

$$(3.1) \quad Q(w) = \langle \psi, w \rangle, \quad \forall w \in \mathcal{W},$$

for some fixed $\psi \in \mathcal{W}$. The QoI is then,

$$(3.2) \quad Q(u) = \langle \psi, u \rangle.$$

For example, in (2.13), $\langle \psi, u \rangle = (\Psi, U)$, that is the inner-product is the L^2 inner product. The aim of the *a posteriori* analysis is to compute the error in the QoI, $Q(u) - Q(u_h) = \langle \psi, u \rangle - \langle \psi, u_h \rangle = \langle \psi, e \rangle$. We briefly describe the analysis for linear problems in §3.1 and then consider nonlinear problems in §3.2.

3.1. Linear variational problems. We consider the problem of evaluating (3.2) where u is the solution to the linear variational problem: find $u \in \mathcal{V}$ such that

$$(3.3) \quad a(u, v) = \langle f, v \rangle, \quad \forall v \in \mathcal{V},$$

where $a : \mathcal{V} \times \mathcal{V} \rightarrow \mathbb{R}$ is a bilinear form. We then define the adjoint bilinear form $a^* : \mathcal{V} \times \mathcal{V} \rightarrow \mathbb{R}$ as the unique bilinear form satisfying

$$(3.4) \quad a^*(w, v) = a(v, w), \quad \forall w, v \in \mathcal{V},$$

see [39, 10]. If ϕ solves the dual problem: find $\phi \in \mathcal{V}$ such that

$$(3.5) \quad a^*(\phi, v) = \langle \psi, v \rangle, \quad \forall v \in \mathcal{V},$$

then we have the following error representation.

THEOREM 3.1. *The error in the QoI (3.2) is represented as $\langle \psi, e \rangle = \langle f, \phi \rangle - a(u_h, \phi)$, where u is the solution to (3.3), u_h is a numerical approximation, $e = u - u_h$ and ϕ is the solution to (3.5).*

Proof. The proof is a straightforward computation,

$$(3.6) \quad \langle \psi, e \rangle = a^*(\phi, e) = a(e, \phi) = a(u, \phi) - a(u_h, \phi) = \langle f, \phi \rangle - a(u_h, \phi). \quad \square$$

Note from the proof above that a simple yet important property of the adjoint bilinear form $a^*(\cdot, \cdot)$ is,

$$(3.7) \quad a^*(v, e) = a(u, v) - a(u_h, v),$$

for $w \in \mathcal{V}$. We will use this property in motivation the analysis for nonlinear problems in §3.2.

3.2. Nonlinear variational problems. Again, our goal is to evaluate (3.2) where now u is the solution to the *nonlinear* variational problem: find u in \mathcal{V} such that

$$(3.8) \quad \mathcal{N}(u, v) = \langle f, v \rangle, \quad \forall v \in \mathcal{V},$$

and $\mathcal{N} : \mathcal{V} \times \mathcal{V} \rightarrow \mathbb{R}$ is linear in the second argument but may be nonlinear in the first argument. There is no straightforward definition of an adjoint operator corresponding to a nonlinear problem. However, a common choice useful for various kinds of analysis is based on linearization [53, 52, 21, 18, 16, 33]. This choice enables the definition of an adjoint bilinear form $\overline{\mathcal{N}}^*(\cdot, \cdot)$ which satisfies the useful property,

$$(3.9) \quad \overline{\mathcal{N}}^*(v, e) = \mathcal{N}(u, v) - \mathcal{N}(u_h, v),$$

for all $v \in \mathcal{V}$. This property is inspired by (3.7).

We now present a specific case of this analysis such the problem (3.8) mimics the setup of the exact penalty problem in (2.6). Let $\mathcal{V} = \prod_{i=1}^n \mathcal{V}_i$ and $\mathcal{W} = \prod_{i=1}^n \mathcal{W}_i$ be product spaces of Hilbert spaces such that \mathcal{V}_i is a dense subspace of \mathcal{W}_i for each i . The left hand side in problem (3.8) is now more specifically given by

$$(3.10) \quad \mathcal{N}(v, w) = \sum_{i=1}^m \langle N_i(v), w_{\ell_i} \rangle + a(v, w),$$

where $a(\cdot, \cdot)$ is a bilinear form, $\ell_i \in \{1, \dots, n\}$ and $N_i : \mathcal{V} \rightarrow \mathcal{W}_{\ell_i}$ are nonlinear operators. For a solution/approximation pair (u/u_h) to (3.8), define the matrix $\overline{\mathcal{J}}$, where each entry $\overline{\mathcal{J}}_{ij} : \mathcal{V}_j \rightarrow \mathcal{W}_{\ell_i}$ is given by

$$(3.11) \quad \overline{\mathcal{J}}_{ij} v_j = \int_0^1 \frac{\partial N_i}{\partial u_j}(su + (1-s)u_h) ds v_j,$$

where $v_j \in \mathcal{V}_j$ and $\frac{\partial N_i}{\partial u_j}(\cdot)$ denotes the partial derivative of N_i with respect to the argument u_j . Define the linearized operator $\bar{N}_i : \mathcal{V} \rightarrow \mathcal{W}_{\ell_i}$ by

$$(3.12) \quad \begin{aligned} \bar{N}_i v &= \int_0^1 \frac{\partial N_i}{\partial u}(su + (1-s)u_h) ds \cdot v \\ &= \sum_{j=1}^n \int_0^1 \frac{\partial N_i}{\partial u_j}(su + (1-s)u_h) ds v_j = \sum_{j=1}^n \bar{\mathcal{J}}_{ij} v_j, \end{aligned}$$

for $v \in \mathcal{V}$. Now since each \bar{N}_i is linear, we may define the bilinear forms, $\bar{v}_i : \mathcal{V} \times \mathcal{V} \rightarrow \mathbb{R}$, by

$$(3.13) \quad \bar{v}_i(v, w) = \langle \bar{N}_i v, w_{\ell_i} \rangle = \left\langle \sum_{j=1}^n \bar{\mathcal{J}}_{ij} v_j, w_{\ell_i} \right\rangle = \sum_{j=1}^n \langle \bar{\mathcal{J}}_{ij} v_j, w_{\ell_i} \rangle,$$

for $v, w \in \mathcal{V}$. Define $\bar{v}_i^*(v, w) = \bar{v}_i(w, v)$, and adjoint operators $\bar{\mathcal{J}}_{ij}^*$ to $\bar{\mathcal{J}}_{ij}$ satisfying

$$(3.14) \quad \langle \bar{\mathcal{J}}_{ij} w, v \rangle = \langle w, \bar{\mathcal{J}}_{ij}^* v \rangle$$

for $w \in \mathcal{V}_j$ and $v \in \mathcal{V}_{\ell_i}$. Hence, we can also write using the definition (3.13),

$$\bar{v}_i^*(v, w) = \sum_{j=1}^n \langle w_j, \bar{\mathcal{J}}_{ij}^* v_{\ell_i} \rangle.$$

for $v, w \in \mathcal{V}$. Also since $a(\cdot, \cdot)$ in (3.10) is a bilinear form, we have from the definition (3.4) that $a^*(w, v) = a(v, w)$ for $v, w \in \mathcal{V}$. With these definitions in mind, we further define a composite adjoint bilinear form, $\bar{\mathcal{N}}^* : \mathcal{V} \times \mathcal{V} \rightarrow \mathbb{R}$, as

$$(3.15) \quad \bar{\mathcal{N}}^*(v, w) = \sum_{i=1}^m \bar{v}_i^*(v, w) + a^*(v, w) = \sum_{i=1}^m \sum_{j=1}^n \langle w_j, \bar{\mathcal{J}}_{ij}^* v_{\ell_i} \rangle + a^*(v, w),$$

for $u, v \in \mathcal{V}$. Then if $\phi \in \mathcal{V}$ solves the dual problem,

$$(3.16) \quad \bar{\mathcal{N}}^*(\phi, v) = \langle \psi, v \rangle, \forall v \in \mathcal{V},$$

we then have the following abstract error representation.

THEOREM 3.2. *The error in the QoI (3.2) is represented as $\langle \psi, e \rangle = \langle f, \phi \rangle - \mathcal{N}(u_h, \phi)$ where u is the solution to (3.8), u_h is a numerical approximation of u , $e = u - u_h$, and ϕ is the solution to (3.16).*

Proof. We compute, starting by replacing v by e in (3.16),

$$\begin{aligned}
\langle \psi, e \rangle &= \overline{\mathcal{N}}^*(\phi, e) = \sum_{i=1}^m \sum_{j=1}^n \langle e_j, \overline{\mathcal{J}}_{ij}^* \phi_{\ell_i} \rangle + a^*(\phi, e) \\
&= \sum_{i=1}^m \sum_{j=1}^n \langle \overline{\mathcal{J}}_{ij} e_j, \phi_{\ell_i} \rangle + a(e, \phi) \\
&= \sum_{i=1}^m \langle \overline{N}_i e, \phi_{\ell_i} \rangle + a(e, \phi) \\
&= \sum_{i=1}^m \langle N_i(u) - N_i(u_h), \phi_{\ell_i} \rangle + a(u, \phi) - a(u_h, \phi) \\
&= \sum_{i=1}^m \langle N_i(u), \phi_{\ell_i} \rangle + a(u, \phi) - \sum_{i=1}^m \langle N_i(u_h), \phi_{\ell_i} \rangle - a(u_h, \phi) \\
&= \mathcal{N}(u, \phi) - \mathcal{N}(u_h, \phi) = \langle f, \phi \rangle - \mathcal{N}(u_h, \phi). \quad \square
\end{aligned}$$

The main result of this theorem is that computing the adjoint to a nonlinear form is reduced to computing the adjoint for the averaged entries, $\overline{\mathcal{J}}_{ij}$.

4. *A posteriori* error estimate for the MHD equations. The analysis in §3.2 applies directly to the MHD equations. The inner product $\langle \cdot, \cdot \rangle$ of the last section is represented by the $[L^2(\Omega)]^{2d+1}$ inner product (\cdot, \cdot) . The linear and nonlinear terms in the exact penalty weak form (2.6) are mapped to match (3.10). The mapping between the abstract formulation and MHD equation is shown in Table 1.

Abstract	MHD	Abstract	MHD	Abstract	MHD
$\langle \cdot, \cdot \rangle$	(\cdot, \cdot)	$\langle f, v \rangle$	(\mathbf{f}, \mathbf{v})	v_3	$V_3 \equiv q$
m	3	u_1	$U_1 \equiv \mathbf{u}$	$\overline{\mathcal{J}}_{11}^*$	$\overline{\mathcal{Z}}_{\mathbf{u}}^*$
\mathcal{N}	\mathcal{N}_{EP}	u_2	$U_2 \equiv \mathbf{b}$	$\overline{\mathcal{J}}_{12}^*$	$\overline{\mathcal{Z}}_{\mathbf{b}}^*$
u	U	u_3	$U_3 \equiv p$	$\overline{\mathcal{J}}_{21}^*$	$\overline{\mathcal{Y}}^*$
v	V	v_1	$V_1 \equiv \mathbf{v}$	$\overline{\mathcal{J}}_{31}^*$	$\overline{\mathcal{C}}^*$
N_i	$N_{EP,i}$	v_2	$V_2 \equiv \mathbf{c}$	a	a_{EP}
(a)		(b)		(c)	

Table 1: Mapping between the abstract framework in §3 and the MHD equation in §4. \mathcal{N}_{EP} is given in (4.1), $N_{EP,i}$ in (4.2), a_{EP} in (4.3) and $\overline{\mathcal{Z}}_{\mathbf{u}}^*$, $\overline{\mathcal{Z}}_{\mathbf{b}}^*$, $\overline{\mathcal{Y}}^*$, $\overline{\mathcal{C}}^*$ are given in (4.4).

For the exact penalty weak form, we have that

$$(4.1) \quad \mathcal{N}_{EP}(U, V) = \sum_{i=1}^3 (N_{EP,i}(U), V_{\ell_i}) + a_{EP}(U, V),$$

where

$$(4.2) \quad \begin{aligned} (N_{EP,1}(U), V_2) &= (\mathcal{Z}(\mathbf{u}, \mathbf{b}), \mathbf{c}), \\ (N_{EP,2}(U), V_1) &= (\mathcal{Y}(\mathbf{b}), \mathbf{v}), \\ (N_{EP,3}(U), V_1) &= (\mathcal{C}(\mathbf{u}), \mathbf{v}), \end{aligned}$$

$\mathcal{Z}, \mathcal{Y}, \mathcal{C}$ are in turn defined in (2.8), and

$$(4.3) \quad \begin{aligned} a_{EP}(U, V) &= \frac{1}{\text{Re}}(\nabla \mathbf{u}, \nabla \mathbf{v}) - (p, \nabla \cdot \mathbf{v}) + (q, \nabla \cdot \mathbf{u}) \\ &\quad + \frac{\kappa}{\text{Re}_m}(\nabla \times \mathbf{b}, \nabla \times \mathbf{c}) + \frac{\kappa}{\text{Re}_m}(\nabla \cdot \mathbf{b}, \nabla \cdot \mathbf{c}). \end{aligned}$$

The entries $\overline{\mathcal{J}}_{11}^* V_2 = \overline{\mathcal{Z}}_{\mathbf{u}}^* \mathbf{c}$, $\overline{\mathcal{J}}_{12}^* V_2 = \overline{\mathcal{Z}}_{\mathbf{b}}^* \mathbf{c}$, $\overline{\mathcal{J}}_{21}^* V_1 = \overline{\mathcal{Y}}^* \mathbf{v}$ and $\overline{\mathcal{J}}_{31}^* V_1 = \overline{\mathcal{C}}^* \mathbf{v}$ are,

$$(4.4) \quad \begin{aligned} \overline{\mathcal{Z}}_{\mathbf{u}}^* \mathbf{c} &= \frac{1}{2}(\mathbf{u} + \mathbf{u}_h) \times (\nabla \times \mathbf{c}), \\ \overline{\mathcal{Z}}_{\mathbf{b}}^* \mathbf{c} &= -\frac{1}{2}(\mathbf{b} + \mathbf{b}_h) \times (\nabla \times \mathbf{c}), \\ \overline{\mathcal{Y}}^* \mathbf{v} &= \frac{1}{2}(-(\nabla \times (\mathbf{b} + \mathbf{b}_h) \times \mathbf{v}) + \nabla \times ((\mathbf{b} + \mathbf{b}_h) \times \mathbf{v})), \\ \overline{\mathcal{C}}^* \mathbf{v} &= \frac{1}{2}((\nabla \mathbf{u} + \nabla \mathbf{u}_h)^T \mathbf{v} - ((\mathbf{u} + \mathbf{u}_h) \cdot \nabla) \mathbf{v}) - (\nabla \cdot (\mathbf{u} + \mathbf{u}_h)) \mathbf{v}, \end{aligned}$$

while the remaining $\overline{\mathcal{J}}_{ij}^*$ entries are zero. The details of the derivation are given in §6.1.

4.1. Adjoint problem for incompressible MHD. We are now prepared to pose a weak adjoint problem corresponding to exact penalty primal problem (2.6). Based on (4.1), (4.4) and (3.16), the weak dual problem is therefore be stated as: find $\Phi = (\phi, \beta, \pi) \in \mathcal{P}$ such that

$$(4.5) \quad \overline{\mathcal{N}}_{EP}^*(\Phi, V) = (\Psi, V), \quad \forall V = (\mathbf{v}, \mathbf{c}, q) \in \mathcal{P},$$

with

$$(4.6) \quad \begin{aligned} \overline{\mathcal{N}}_{EP}^*(\Phi, V) &= \frac{1}{\text{Re}}(\nabla \phi, \nabla \mathbf{v}) + (\overline{\mathcal{C}}^* \phi, \mathbf{v}) + (\nabla \cdot \mathbf{v}, \pi) - (\nabla \cdot \phi, q) \\ &\quad + \frac{\kappa}{\text{Re}_m}(\nabla \times \beta, \nabla \times \mathbf{c}) + \frac{\kappa}{\text{Re}_m}(\nabla \cdot \beta, \nabla \cdot \mathbf{c}) \\ &\quad - \kappa(\overline{\mathcal{Y}}^* \phi, \mathbf{c}) - \kappa(\overline{\mathcal{Z}}_{\mathbf{u}}^* \beta, \mathbf{v}) - \kappa(\overline{\mathcal{Z}}_{\mathbf{b}}^* \beta, \mathbf{c}). \end{aligned}$$

Here recall that Ψ is defined by (2.13). The forms of the linear operators $\overline{\mathcal{C}}^*$, $\overline{\mathcal{Y}}^*$, $\overline{\mathcal{Z}}_{\mathbf{u}}^*$ and $\overline{\mathcal{Z}}_{\mathbf{b}}^*$ are given in (4.4). We discuss the well-posedness of the adjoint problem (4.5) in §6.2.

4.2. Error representation. In order to discuss an error representation we need to make the following definition

DEFINITION 4.1. *Define the monolithic error by $E = [\mathbf{e}_{\mathbf{u}}, \mathbf{e}_{\mathbf{b}}, e_p]^T$ with component errors*

$$(4.7) \quad \mathbf{e}_{\mathbf{u}} = \mathbf{u} - \mathbf{u}_h, \quad \mathbf{e}_{\mathbf{b}} = \mathbf{b} - \mathbf{b}_h, \quad e_p = p - p_h.$$

where $(\mathbf{u}, \mathbf{b}, p) \in \mathcal{P}$ is the solution to (2.6) and $(\mathbf{u}_h, \mathbf{b}_h, p_h) \in \mathcal{P}_h$ is the solution to (2.12).

We then have the following error representation.

THEOREM 4.2 (Error representation for exact penalty). *The error in the numer-*

ical approximation of the QoI (2.13) satisfies

$$\begin{aligned}
(\Psi, E) = (\mathbf{f}, \phi) &- \left[\frac{1}{\text{Re}} (\nabla \mathbf{u}_h, \nabla \phi) + (\mathbf{u}_h \cdot \nabla \mathbf{u}_h, \phi) \right. \\
&- (p_h, \nabla \cdot \phi) + \kappa ((\nabla \times \mathbf{b}_h) \times \mathbf{b}_h, \phi) + (\nabla \cdot \mathbf{u}_h, \pi) \\
&+ \frac{\kappa}{\text{Re}_m} (\nabla \times \mathbf{b}_h, \nabla \times \boldsymbol{\beta}) + \kappa (\nabla \times (\mathbf{u}_h \times \mathbf{b}_h), \boldsymbol{\beta}) \\
&\left. + \frac{\kappa}{\text{Re}_m} (\nabla \cdot \mathbf{b}_h, \nabla \cdot \boldsymbol{\beta}) \right],
\end{aligned}$$

where $\Phi = (\phi, \boldsymbol{\beta}, \pi)$ is defined in (4.5).

Proof. By Theorem 3.2,

$$(\Psi, E) = \overline{\mathcal{N}}_{EP}^*(\Phi, E) = \mathcal{N}_{EP}(U, \Phi) - \mathcal{N}_{EP}(U_h, \Phi) = (\mathbf{f}, \phi) - \mathcal{N}_{EP}(U_h, \Phi). \quad \square$$

4.3. Non-homogeneous boundary conditions for the MHD system. The analysis above easily extends to the case of non-homogeneous boundary conditions, i.e. when \mathbf{g} or \mathbf{q} are not identically zero. First assume that the numerical solution U_h satisfies the non-homogeneous conditions exactly. That is, $\mathbf{u} = \mathbf{u}_h = \mathbf{g}$ and $\mathbf{b} \times \mathbf{n} = \mathbf{b}_h \times \mathbf{n} = \mathbf{q} \times \mathbf{n}$ on $\partial\Omega$. Then, although neither the true solution U nor the numerical solution U_h belong to \mathcal{P} , the error E defined in Definition 4.1 satisfies homogeneous boundary conditions and hence belongs to \mathcal{P} . Thus, the error analysis in the previous section applies directly in this case.

On the other hand, if U_h belongs to $\mathcal{P}_h \setminus \mathcal{P}$, then in general U_h does not satisfy the non-homogeneous boundary conditions exactly. Hence we consider the splitting of the numerical solutions as,

$$(4.8) \quad U_h = U_h^0 + U^d,$$

where $U_h^0 \in \mathcal{P}_h$ solves,

$$(4.9) \quad \mathcal{N}_{EP}(U_h, V_h) = \mathcal{N}_{EP}(U_h^0 + U^d, V_h) = (F, V_h), \quad \forall V_h \in \mathcal{P}_h,$$

and U^d is a known function that satisfies the non-homogeneous boundary conditions accurately. That is, the unknown is now U_h^0 and the numerical solution U_h is formed through the sum in (4.8). In this article the function U^d is approximated through a finite element space of much higher dimension than \mathcal{P}_h to capture the boundary conditions accurately and hence minimize discretization error. An alternate approach is to represent U^d in the same space as U_h^0 and then quantify the error due to this approximation, for example see [16].

4.4. Error estimate and contributions. The error representation in Theorem 4.2 requires the exact solution $\Phi = (\phi, \boldsymbol{\beta}, \pi) \in \mathcal{P}$ of (4.5). Moreover, the adjoint form (4.6) is linearized around the true solution U and the approximate solution U_h . In practice, the adjoint solution itself must be approximated in a finite element space $\mathcal{W}^h \subset \mathcal{P}$ and is linearized only around the numerical solution. Let this approximation to the adjoint be denoted by $\Phi_h = (\phi_h, \boldsymbol{\beta}_h, \pi_h) \in \mathcal{W}^h$. This approximation leads to an error estimate from the error representation in Theorem 4.2. Let this error estimate be denoted by η . That is, $\eta \approx (\Psi, E)$ such that,

$$(4.10) \quad \eta = E_{mom} + E_{con} + E_M,$$

where,

$$\begin{aligned}
 E_{mom} &= (\mathbf{f}, \phi_h) - \left(\frac{1}{\text{Re}} (\nabla \mathbf{u}_h, \nabla \phi_h) + ((\mathbf{u}_h \cdot \nabla) \mathbf{u}_h, \phi_h) - (p_h, \nabla \cdot \phi_h) \right. \\
 &\quad \left. + \kappa ((\nabla \times \mathbf{b}_h) \times \mathbf{b}_h, \phi_h) \right), \\
 (4.11) \quad E_{con} &= -(\nabla \cdot \mathbf{u}_h, \pi_h), \\
 E_M &= -\frac{\kappa}{\text{Re}_m} (\nabla \times \mathbf{b}_h, \nabla \times \beta_h) + \kappa (\nabla \times (\mathbf{u}_h \times \mathbf{b}_h), \beta_h) \\
 &\quad - \frac{\kappa}{\text{Re}_m} (\nabla \cdot \mathbf{b}_h, \nabla \cdot \beta_h).
 \end{aligned}$$

Here E_{mom} , E_{con} and E_M represent the momentum error contribution, the continuity error contribution and the magnetic error contribution respectively.

To obtain an accurate error estimate we choose \mathcal{W}^h to be of much higher dimension than \mathcal{P}_h as is standard in adjoint based *a posteriori* error estimation [34, 28, 25, 20, 19, 34, 22, 15, 9]. Moreover, the inaccuracy caused by substituting the numerical solution in place of true solution in the adjoint form is of higher order and shown to decrease in the limit of refined discretization [34, 23].

5. Numerical results. In this section we present numerical results to verify the accuracy of the error estimate (4.10) and the utility of the error contributions in (4.11). The effectivity ratio, denoted *Eff.*, characterizes how well the error estimate approximates the true error,

$$(5.1) \quad \text{Eff.} = \frac{\text{Error estimate}}{\text{True error}} = \frac{\eta}{(\Psi, E)}.$$

The closer the effectivity is to 1, the better the error estimate provided by our method.

We present two numerical examples here, the Hartmann problem in §5.1 which admits an analytic solution, and the magnetic lid driven cavity §5.2. Since there is no closed form solution for the magnetic lid driven cavity, we use as reference a high order/fine mesh solution to provide a high accuracy estimate for the true error. All the following computations were carried out using the finite element package *Dolfin* in the *FEniCS* suite [7, 50, 51].

For all experiments, we chose different polynomial orders of Lagrange spaces for the product space \mathcal{P}_h and choose the adjoint space \mathcal{W}^h such that it is one higher polynomial degree in each variable. The computational domain for all problems is chosen to be a unit length square, $\Omega := [-\frac{1}{2}, \frac{1}{2}]^2 \subset \mathbb{R}^2$. The mesh is a simplicial uniform mesh with the total number of elements denoted by *#Elements*.

5.1. Hartmann flow in two dimensions. Our first results concern the so-called Hartmann problem [63]. This problem models the one-dimensional flow of a conducting fluid in a channel and forms both a momentum boundary layer (viscous boundary layer), and a layer formed by the diffusion of the magnetic field that influences the flow due to the Lorentz force (a Hartmann layer). In this case we take consider a square channel as the computational domain, however the analytic solution is only a one-dimensional profile, as described in the beginning of the section. This

problem admits an analytic solution [57], $\mathbf{u} = [u_x, 0]^T$, $\mathbf{b} = [b_x, 1]^T$, p where

$$(5.2a) \quad u_x(y) = \frac{G \operatorname{Re}(\cosh(H_a/2) - \cosh(H_a y))}{2H_a \sinh(H_a/2)},$$

$$(5.2b) \quad B_x(y) = \frac{G(\sinh(H_a y) - 2 \sinh(H_a/2)y)}{2\kappa \sinh(H_a/2)},$$

$$(5.2c) \quad p(x) = -Gx - \kappa B_x^2/2,$$

and $G = -\frac{dp}{dx}$ is an arbitrary pressure drop that we choose to normalize the maximum velocity $|u_x(y)|$ to 1.

5.1.1. Problem parameters and QoI. The values of the nondimensionalized constants are chosen as follows: $\operatorname{Re} = 16$, $\operatorname{Re}_m = 16$, $\kappa = 1$ which produce a Hartmann number of $H_a = 16$. The QoI is chosen as the average velocity across the flow over a slice. To this end, define

$$(5.3) \quad \Omega_c := \left[-\frac{1}{4}, \frac{1}{2}\right] \times \left[-\frac{1}{4}, \frac{1}{4}\right]$$

and consequently $\mathbb{1}_{\Omega_c}$ the characteristic function on Ω_c . We choose Ψ to be $\Psi = [\mathbb{1}_{\Omega_c}, 0, 0, 0]^T$ so that the QoI (2.13) thus reduces to

$$(5.4) \quad (\Psi, U) = (\mathbb{1}_{\Omega_c}, u_x).$$

This has a physical interpretation of the capturing the flow rate across this slice of the channel, Ω_c .

5.1.2. Numerical results and discussion. The error contributions of (4.10) as well as effectivity ratios using different order polynomial spaces are presented in Table 2, Table 3, Table 4, and Table 5. The effectivity ratio in tables Table 2 and Table 3 is quite close to 1 indicating the accuracy of the error estimate. The error estimate in Table 4 is not as accurate due to linearization error incurred by replacing the true solution by the approximate solution in the definition of the adjoint as discussed in §4.4. This may be verified by linearizing the adjoint weak form around both the true (which we know for this example) and the approximate solutions. These results are shown in Table 5 and now the error estimate is again accurate.

In Table 2 we use the lowest order tuple of Lagrange spaces, $(\mathbb{P}^2, \mathbb{P}^1, \mathbb{P}^1)$ for the variables $(\mathbf{u}, \mathbf{b}, p)$. In this case, the error is largely dominated by the contributions E_{con} and E_M . We greatly reduce the error in E_M by using a higher degree Lagrange space, \mathbb{P}^2 , for \mathbf{b} as demonstrated in table Table 3. However, this does not reduce the magnitude of the total error much (about 5%) which is still dominated by the contribution E_{con} . The contribution E_{con} is not significantly affected by the finite dimensional space for \mathbf{b} . Now finally, in Table 4 we use a higher order tuple $(\mathbb{P}^3, \mathbb{P}^2, \mathbb{P}^2)$ for $(\mathbf{u}, \mathbf{b}, p)$ and the total error drops by two orders of magnitude.

5.2. Magnetic Lid Driven Cavity.

5.2.1. Regularization and solution method. The magnetic lid driven cavity is another common benchmark problem for verifying MHD codes [57, 60]. However, the standard lid velocity is discontinuous and therefore obtains at most $H^{1/2-\varepsilon}$ regularity in two dimensions with $\varepsilon > 0$. By the converse of the trace theorem and the Sobolev inequality [27, 13], the solution u_x cannot obtain H^1 regularity on the interior. Indeed, in this situation, we do not even have well-posedness of the primal

# Elements	True Error	Eff.	E_{mom}	E_{con}	E_M
1600	2.76e-04	1.00	4.53e-06	-2.28e-04	5.00e-04
6400	6.98e-05	1.00	1.29e-06	-6.23e-05	1.31e-04
14400	3.11e-05	1.00	6.05e-07	-2.86e-05	5.91e-05
25600	1.75e-05	1.00	3.49e-07	-1.63e-05	3.35e-05

Table 2: Error in $(u_x, \mathbb{1}_{\Omega_c})$ for the Hartmann problem §5.1, with $\mathbb{1}_{\Omega_c} = [-\frac{1}{4}, \frac{1}{2}] \times [-\frac{1}{4}, \frac{1}{4}]$. The finite dimensional space here is $(\mathbb{P}^2, \mathbb{P}^1, \mathbb{P}^1)$ for $(\mathbf{u}, \mathbf{b}, p)$.

# Elements	True Error	Eff.	E_{mom}	E_{con}	E_M
1600	-2.25e-04	1.02	1.08e-06	-2.27e-04	-4.79e-06
6400	-6.13e-05	1.04	1.04e-06	-6.23e-05	-2.18e-06
14400	-2.81e-05	1.04	5.98e-07	-2.86e-05	-1.13e-06
25600	-1.60e-05	1.04	3.76e-07	-1.64e-05	-6.81e-07

Table 3: Error in $(u_x, \mathbb{1}_{\Omega_c})$ for the Hartmann problem §5.1. The finite dimensional space here is $(\mathbb{P}^2, \mathbb{P}^2, \mathbb{P}^1)$ for $(\mathbf{u}, \mathbf{b}, p)$.

# Elements	True Error	Eff.	E_{mom}	E_{con}	E_M
1600	1.23e-06	1.21	3.97e-07	-4.15e-06	5.24e-06
6400	1.46e-07	1.47	9.23e-08	-5.07e-07	6.29e-07
14400	4.97e-08	1.63	3.84e-08	-1.40e-07	1.83e-07
25600	2.47e-08	1.73	2.07e-08	-5.44e-08	7.64e-08

Table 4: Error in $(u_x, \mathbb{1}_{\Omega_c})$ for the Hartmann problem §5.1. The finite dimensional space here is $(\mathbb{P}^3, \mathbb{P}^2, \mathbb{P}^2)$ for $(\mathbf{u}, \mathbf{b}, p)$. Here, we approximate the true solution with the computed solution which results in linearization error. For this accurate a solution, this deteriorates the quality of the estimate which in turn results in a efficiency further from 1. This is confirmed in Table 5 where we use the true solution and the effectivity is again close to 1.

2d Elem.	True Error	Eff.	E_{mom}	E_{con}	E_M
1600	1.23e-06	1.00	2.75e-07	-4.39e-06	5.34e-06
6400	1.46e-07	1.00	5.97e-08	-5.60e-07	6.46e-07
14400	4.97e-08	1.00	2.35e-08	-1.63e-07	1.89e-07
25600	2.47e-08	1.00	1.22e-08	-6.65e-08	7.90e-08

Table 5: Error in $(u_x, \mathbb{1}_{\Omega_c})$ for the Hartmann problem, §5.1. The finite dimensional space here is $(\mathbb{P}^3, \mathbb{P}^2, \mathbb{P}^2)$ for $(\mathbf{u}, \mathbf{b}, p)$. No linearization error is present here because we use the true solution in the definition of the adjoint.

problem, so there is not real hope for error analysis. This issue has been address in a purely fluid context [43, 47]. In both cases, a regularization of the lid velocity is proposed to mitigate theoretical issues (in the former) and the ability to achieve higher Reynold's numbers (in the latter). In this work, we use a similar regularization

to the one proposed in [47], a polynomial regularization of the lid velocity,

$$u_{top}(x) = C \left(x - \frac{1}{2}\right)^2 \left(x + \frac{1}{2}\right)^2,$$

with C chosen such that

$$\int_{-1/2}^{1/2} u_{top}(x) dx = 1.$$

The boundary conditions are imposed as $\mathbf{g}(x, 0.5) = [u_{top}, 0]^T$ on the top face and zero on the rest of the boundary. The boundary conditions for the magnetic field are $\mathbf{q} = [-1, 0]^T$ so that $\mathbf{b} \times \mathbf{n} = [-1, 0]^T \times \mathbf{n}$ on $\partial\Omega$. To get a qualitative measure of the validity of the regularized problem, we show plot of the velocity profile for a fixed Reynold's number $\text{Re} = 5000$ and varying magnetic Reynold's numbers Re_m in Figure 1. These plots are qualitatively similar to Figure 1 in [57] (for which an un-regularized lid velocity is used), which gives a good indication that the regularized version produces qualitatively similar features.

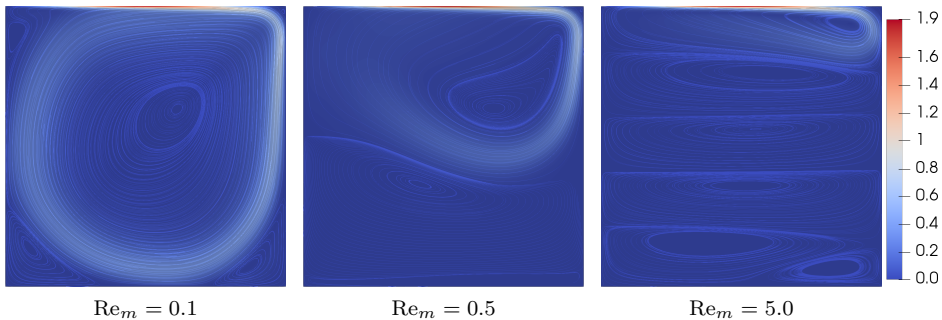


Fig. 1: Plots of the $\|\mathbf{u}\|_{\mathbb{R}^d}$ for the lid driven cavity §5.2 with added streamlines. We use a normalization on the lid velocity over a variety of magnetic Reynold's numbers, Re_m . The other nondimensionalized parameters $\text{Re} = 5000, \kappa = 1$ for all of these plots.

Furthermore, since Newton's method requires a good initial guess for this problem, we use a homotopic sequence of initial guesses to achieve convergence to high Re . Specifically we run the problem for a moderate value of $\text{Re} = 200$ for example, and then use the solution produced by the solver as the initial guess for a larger value e.g. $\text{Re} = 1000$ until we have achieved the desired value. Figure 2 shows the intermediate values in this sequence to solve a problem with $\text{Re} = 1000$.

5.2.2. Problem parameters and results. We consider our QoI (2.13) with $\Psi = [0, 0, 0, \mathbb{1}_{\Omega_c}, 0]^T$ where now

$$(5.5) \quad \Omega_c := \left[-\frac{1}{4}, \frac{1}{4}\right] \times \left[0, \frac{1}{2}\right],$$

so that the QoI $(\Psi, U) = (\mathbb{1}_{\Omega_c}, b_y)$ gives a measure of the induced magnetic field in the upper middle half of the box. See Figure 2 for plots of the induced field b_y as a function of Reynold's number Re .

Since there is no analytic solution for this problem, we compute solution on a 400×400 mesh in the space $(\mathbb{P}^3, \mathbb{P}^2, \mathbb{P}^2)$ for $(\mathbf{u}, \mathbf{b}, p)$. We consider the QoI obtained

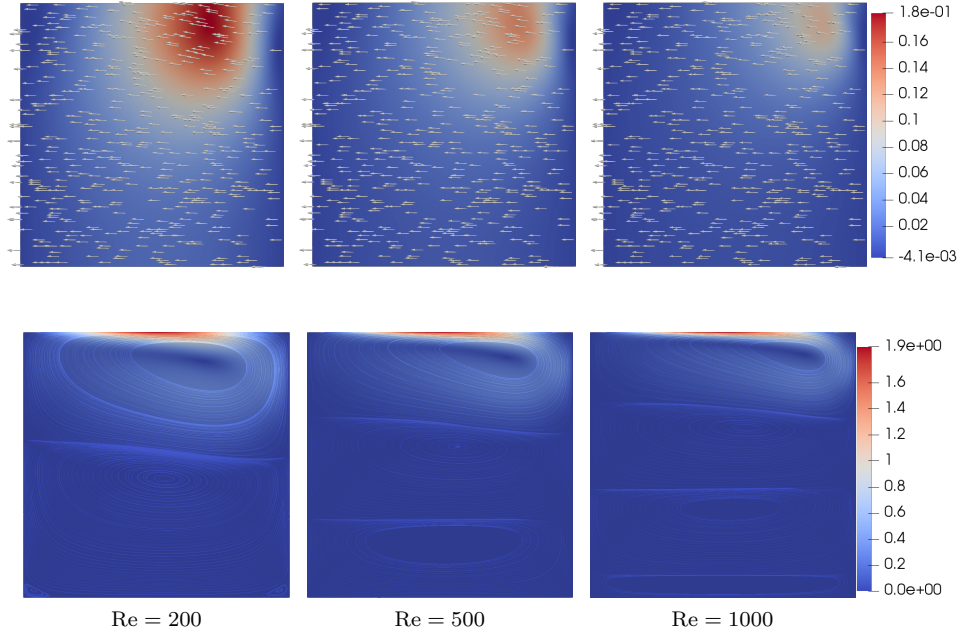


Fig. 2: Demonstrating the homotopy parameter strategy to achieve high fluid Reynolds numbers as described in §5.2. The other nondimensionalized parameters $Re_m = 5.0, \kappa = 1$ for all of these plots. The top row is colored according to the b_y and with the arrows representing the vector \mathbf{b} . The bottom row is colored according to $\|\mathbf{u}\|_{\mathbb{R}^d}$, with added streamlines.

from this very high resolution reference solution as the true solution to compute the error in the denominator of the effectivity ratio (5.1). The effectivity ratio and error contributions for $Re = 1000$ and $Re = 2000$ are shown in Tables 6, 7, 8 and 9. The error estimate η is deemed accurate since all effectivity ratios are close to 1.

We first study the lowest order case, namely using the space $(\mathbb{P}^2, \mathbb{P}^1, \mathbb{P}^1)$ for $(\mathbf{u}, \mathbf{b}, p)$ in Table 6 where $Re = 1000$ and Table 8 where $Re = 2000$. For both $Re = 2000$ and $Re = 1000$, the error contributions are not drastically different in magnitude, and become even more similar as the mesh is refined. We also note that all contributions, and in particular the true error, are larger in magnitude for the case $Re = 2000$.

For the next experiment, we consider a higher order space for the velocity pair (\mathbf{u}, p) namely $(\mathbb{P}^3, \mathbb{P}^1, \mathbb{P}^2)$ for $(\mathbf{u}, \mathbf{b}, p)$ in Table 7 for $Re = 1000$ and Table 9 for $Re = 2000$. In both cases, the error is now dominated by the contribution E_M . The case of $Re = 2000$ is particularly interesting, as the error increases as the mesh is refined from 1600 elements to 3600 elements. This seemingly anomalous behavior is explain by examining the error contributions. For $\#Elements = 1600$ we have that $E_{mom} + E_{con}$ has magnitude comparable to that of E_M but opposite sign, and hence there is cancellation of error. For $\#Elements = 3600$, the magnitude of $E_{mom} + E_{con}$ is much less than that of E_M and hence the total error increases as there is less cancellation of error. Hence, adjoint based analysis not only quantifies the error, it

also helps in diagnosing such anomalous behavior.

# Elements	True Error	Eff.	E_{mom}	E_{con}	E_M
1600	-3.93e-05	0.99	-1.05e-05	-2.47e-05	-3.78e-06
3600	-9.50e-06	0.97	-2.23e-06	-5.23e-06	-1.74e-06
6400	-3.41e-06	0.98	-8.12e-07	-1.52e-06	-9.87e-07
10000	-1.61e-06	0.98	-3.64e-07	-5.81e-07	-6.33e-07

Table 6: Error estimates for $(b_y, \mathbb{1}_{\Omega_c})$ for the lid driven cavity §5.2. The finite dimensional space here is $(\mathbb{P}^2, \mathbb{P}^1, \mathbb{P}^1)$ for $(\mathbf{u}, \mathbf{b}, p)$. We use a very high resolution reference solution on a $400 \times 400 = 160000$ element mesh and $(\mathbb{P}^3, \mathbb{P}^2, \mathbb{P}^2)$ elements. The parameters are $\text{Re} = 1000, \text{Re}_m = 0.4, \kappa = 1$.

# Elements	True Error	Eff.	E_{mom}	E_{con}	E_M
1600	-5.37e-06	0.98	-4.65e-07	-9.75e-07	-3.81e-06
3600	-1.95e-06	0.99	-5.49e-08	-1.27e-07	-1.75e-06
6400	-1.03e-06	1.00	-1.06e-08	-2.76e-08	-9.87e-07
10000	-6.45e-07	1.00	-2.89e-09	-8.04e-09	-6.33e-07

Table 7: Error estimates for $(b_y, \mathbb{1}_{\Omega_c})$ for the lid driven cavity §5.2. The finite dimensional space here is $(\mathbb{P}^2, \mathbb{P}^2, \mathbb{P}^1)$ for $(\mathbf{u}, \mathbf{b}, p)$. We use a very high resolution reference solution on a $400 \times 400 = 160000$ element mesh and $(\mathbb{P}^3, \mathbb{P}^2, \mathbb{P}^2)$ elements. The parameters are $\text{Re} = 1000, \text{Re}_m = 0.4, \kappa = 1$.

# Elements	True Error	Eff.	E_{mom}	E_{con}	E_M
1600	-8.01e-05	1.10	-3.65e-05	-5.70e-05	5.63e-06
3600	-2.04e-05	0.98	-5.69e-06	-1.66e-05	2.25e-06
6400	-5.92e-06	0.96	-1.84e-06	-5.06e-06	1.19e-06
10000	-2.07e-06	0.96	-8.17e-07	-1.91e-06	7.41e-07

Table 8: Error estimates for $(b_y, \mathbb{1}_{\Omega_c})$ for the lid driven cavity §5.2. The finite dimensional space here is $(\mathbb{P}^2, \mathbb{P}^1, \mathbb{P}^1)$ for $(\mathbf{u}, \mathbf{b}, p)$. We use a very high resolution reference solution on a $400 \times 400 = 160000$ element mesh and $(\mathbb{P}^3, \mathbb{P}^2, \mathbb{P}^2)$ elements. The parameters are $\text{Re} = 2000, \text{Re}_m = 0.4, \kappa = 1$.

5.3. Illustrative compute time comparison of the primal and adjoint problems. In this section we study CPU times for the Hartmann problem of §5.1 using $(\mathbb{P}^2, \mathbb{P}^1, \mathbb{P}^1)$ for $(\mathbf{u}, \mathbf{b}, p)$. In particular this corresponds to the experiment in Table 2. We compare the CPU time of numerically solving the adjoint problem with solving the discrete forward problem (2.12). The adjoint problem is solved in a higher order space $(\mathbb{P}^3, \mathbb{P}^2, \mathbb{P}^2)$, but since it is linear, it is not obvious how it compares in terms of computational cost to the primal problem. The CPU times are shown in Table 10¹. The CPU time required for the adjoint problem is less in all cases than

¹These experiments were carried out using a dual-socket workstation with two Intel Xeon E5-2687W v2 for a total of 16 physical cores and 32 threads.

# Elements	True Error	Eff.	E_{mom}	E_{con}	E_M
1600	1.31e-06	0.78	-1.58e-06	-3.47e-06	6.08e-06
3600	1.51e-06	0.96	-1.91e-07	-5.29e-07	2.17e-06
6400	1.02e-06	0.98	-3.87e-08	-1.28e-07	1.17e-06
10000	6.94e-07	0.99	-1.07e-08	-4.04e-08	7.38e-07

Table 9: Error estimates for $(b_y, \mathbb{1}_{\Omega_c})$ for the lid driven cavity §5.2. The finite dimensional space here is $(\mathbb{P}^3, \mathbb{P}^2, \mathbb{P}^1)$ for $(\mathbf{u}, \mathbf{b}, p)$. We use an very high resolution reference solution on a $400 \times 400 = 160000$ element mesh and $(\mathbb{P}^3, \mathbb{P}^2, \mathbb{P}^2)$ elements. The parameters are $\text{Re} = 2000, \text{Re}_m = 0.4, \kappa = 1$.

# Elements	Primal solve time (s)	Adjoint solve time (s)
1600	0.73	0.45
6400	3.40	1.62
14400	6.28	4.09
25600	11.70	8.01

Table 10: CPU times for the primal problem (using $(\mathbb{P}^2, \mathbb{P}^1, \mathbb{P}^1)$) and adjoint problem (using $(\mathbb{P}^3, \mathbb{P}^2, \mathbb{P}^2)$) corresponding to the results in Table 2.

the CPU time required for solving the primal problem. We note that these results depend on the choice of linear and nonlinear solvers and preconditioners; here we are simply using Newton's method and direct linear solvers for the primal problems and direct linear solvers for the adjoint problems.

6. Derivation of the weak adjoint and well-posedness. In this section we provide the details of computing the adjoint to exact penalty weak form following the theory in §3. Then we use a standard saddle point argument to demonstrate the well-posedness of this new adjoint problem (4.5). We take inspiration for these proofs from [42]. To simplify notation in this section, we define

$$(6.1) \quad \mathbf{s} := \mathbf{u} + \mathbf{u}_h, \quad \mathbf{t} := \mathbf{b} + \mathbf{b}_h.$$

Finally, we use the notation $\stackrel{(\cdot)}{=}$ and $\stackrel{(\cdot)}{\leq}$ to denote that the equality or inequality is justified by equation (\cdot) .

6.1. Derivation of the weak form of the adjoint. In this section we provide derivation for the primal linearized operators $\bar{\mathcal{J}}_{21}^* = \bar{\mathcal{Y}}^*$, $\bar{\mathcal{J}}_{11}^* = \bar{\mathcal{Z}}_{\mathbf{u}}^*$, $\bar{\mathcal{J}}_{12}^* = \bar{\mathcal{Z}}_{\mathbf{b}}^*$ and $\bar{\mathcal{J}}_{31}^* = \bar{\mathcal{C}}^*$ in (4.4). We first compute the primal linearized operators, $\bar{\mathcal{Y}} = \bar{\mathcal{J}}_{21}$, $\bar{\mathcal{Z}}_{\mathbf{u}} = \bar{\mathcal{J}}_{11}$, $\bar{\mathcal{Z}}_{\mathbf{b}} = \bar{\mathcal{J}}_{12}$ and $\bar{\mathcal{C}} = \bar{\mathcal{J}}_{31}$, using (3.11) and then apply (3.14) to compute the $\bar{\mathcal{J}}_{ij}^*$ s. We have from (3.11) for $\mathbf{d} \in \mathbf{H}_\tau^1(\Omega)$ and $\mathbf{w} \in \mathbf{H}_0^1(\Omega)$,

$$\begin{aligned} \bar{\mathcal{Y}} \mathbf{d} &:= \int_0^1 \frac{\partial \mathcal{Y}}{\partial \mathbf{b}} (\mathbf{s} \mathbf{b} + (1-s) \mathbf{b}_h) \mathbf{d} \, ds, \\ \bar{\mathcal{Z}}_{\mathbf{b}} \mathbf{d} &:= \int_0^1 \frac{\partial \mathcal{Z}}{\partial \mathbf{b}} (\mathbf{s} \mathbf{u} + (1-s) \mathbf{u}_h) \mathbf{d} \, ds, \\ \bar{\mathcal{Z}}_{\mathbf{u}} \mathbf{w} &:= \int_0^1 \frac{\partial \mathcal{Z}}{\partial \mathbf{u}} (\mathbf{s} \mathbf{b} + (1-s) \mathbf{b}_h) \mathbf{w} \, ds. \end{aligned}$$

To this end, we compute

$$\begin{aligned}
\overline{\mathcal{Y}} \mathbf{d} &= \int_0^1 \frac{\partial \mathcal{Y}}{\partial \mathbf{b}} (s\mathbf{b} + (1-s)\mathbf{b}_h) \mathbf{d} \, ds \\
(6.2) \quad &= \int_0^1 [\nabla \times (s\mathbf{b} + (1-s)\mathbf{b}_h)] \times \mathbf{d} + (\nabla \times \mathbf{d}) \times (s\mathbf{b} + (1-s)\mathbf{b}_h) \, ds \\
&= \frac{1}{2} [(\nabla \times (\mathbf{b}_h + \mathbf{b})) \times \mathbf{d} + (\nabla \times \mathbf{d}) \times (\mathbf{b}_h + \mathbf{b})].
\end{aligned}$$

Similarly, for the two $\overline{\mathcal{Z}}$ terms,

$$\begin{aligned}
\overline{\mathcal{Z}}_{\mathbf{b}} \mathbf{d} &= \int_0^1 \frac{\partial \mathcal{Z}}{\partial \mathbf{b}} (s\mathbf{u} + (1-s)\mathbf{u}_h) \mathbf{d} \, ds \\
(6.3) \quad &= \int_0^1 \nabla \times ((s\mathbf{u} + (1-s)\mathbf{u}_h) \times \mathbf{d}) \, ds = \frac{1}{2} [\nabla \times ((\mathbf{u}_h + \mathbf{u}) \times \mathbf{d})].
\end{aligned}$$

An identical procedure produces,

$$(6.4) \quad \overline{\mathcal{Z}}_{\mathbf{u}} \mathbf{w} = \frac{1}{2} [\nabla \times (\mathbf{w} \times (\mathbf{b} + \mathbf{b}_h))].$$

Now, to find the adjoints of these operators, we use (3.14), which in our case involves multiplying by a test function and then isolating the trial function using integration by parts. We also make use of the vector identities in Appendix B.

We are now prepared to compute the adjoint for $\overline{\mathcal{Y}}$. Integrating (6.2) against $\mathbf{v} \in \mathbf{H}_0^1(\Omega)$,

$$\begin{aligned}
(\overline{\mathcal{Y}} \mathbf{d}, \mathbf{v}) &= \frac{1}{2} \int_{\Omega} [(\nabla \times \mathbf{t}) \times \mathbf{d} + (\nabla \times \mathbf{d}) \times \mathbf{t}] \cdot \mathbf{v} \, dx \\
&\stackrel{\text{(B.1a)}}{=} \frac{1}{2} \int_{\Omega} \mathbf{d} \cdot [\mathbf{v} \times (\nabla \times \mathbf{t})] + (\nabla \times \mathbf{d}) \cdot [\mathbf{t} \times \mathbf{v}] \, dx \\
&\stackrel{\text{(B.1b)}}{=} \frac{1}{2} \int_{\Omega} -\mathbf{d} \cdot [(\nabla \times \mathbf{t}) \times \mathbf{v}] + \mathbf{d} \cdot [\nabla \times (\mathbf{t} \times \mathbf{v})] \, dx - \frac{1}{2} \int_{\partial\Omega} \mathbf{d} \cdot [(\mathbf{t} \times \mathbf{v}) \times \mathbf{n}] \, ds \\
&\stackrel{\text{(B.1a)}}{=} \frac{1}{2} \int_{\Omega} -\mathbf{d} \cdot [(\nabla \times \mathbf{t}) \times \mathbf{v}] + \mathbf{d} \cdot [\nabla \times (\mathbf{t} \times \mathbf{v})] \, dx + \frac{1}{2} \int_{\partial\Omega} (\mathbf{t} \times \mathbf{v}) \cdot [\mathbf{d} \times \mathbf{n}] \, ds \\
&\stackrel{\text{(2.4)}}{=} \frac{1}{2} \int_{\Omega} -\mathbf{d} \cdot [(\nabla \times \mathbf{t}) \times \mathbf{v}] + \mathbf{d} \cdot [\nabla \times (\mathbf{t} \times \mathbf{v})] \, dx \stackrel{\text{(4.4)}}{=} (\mathbf{d}, \overline{\mathcal{Y}}^* \mathbf{v}).
\end{aligned}$$

We proceed with computing the adjoint for $\overline{\mathcal{Z}}_{\mathbf{u}}$, with $\mathbf{c} \in \mathbf{H}_\tau^1(\Omega)$,

$$\begin{aligned}
(\overline{\mathcal{Z}}_{\mathbf{u}} \mathbf{w}, \mathbf{c}) &= \frac{1}{2} (\nabla \times (\mathbf{w} \times \mathbf{t}), \mathbf{c}) \\
&\stackrel{\text{(B.1b)}}{=} \frac{1}{2} \int_{\Omega} (\mathbf{w} \times \mathbf{t}) \cdot (\nabla \times \mathbf{c}) \, dx - \frac{1}{2} \int_{\partial\Omega} (\mathbf{w} \times \mathbf{t}) \cdot (\mathbf{c} \times \mathbf{n}) \, ds \\
&\stackrel{\text{(B.1a)}}{=} \frac{1}{2} \int_{\Omega} \mathbf{w} \cdot [\mathbf{t} \times (\nabla \times \mathbf{c})] \, dx - \frac{1}{2} \int_{\partial\Omega} (\mathbf{w} \times \mathbf{t}) \cdot (\mathbf{c} \times \mathbf{n}) \, ds \\
&\stackrel{\text{(2.4)}}{=} \frac{1}{2} \int_{\Omega} \mathbf{w} \cdot [\mathbf{t} \times (\nabla \times \mathbf{c})] \, dx \stackrel{\text{(4.4)}}{=} (\mathbf{w}, \overline{\mathcal{Z}}_{\mathbf{u}}^* \mathbf{c}).
\end{aligned}$$

Finally we compute the adjoint to the linearized operator $\overline{\mathcal{Z}}_b$, again with $\mathbf{c} \in \mathbf{H}_\tau^1(\Omega)$,

$$\begin{aligned}
 (\overline{\mathcal{Z}}_b \mathbf{d}, \mathbf{c}) &= \frac{1}{2} (\nabla \times (\mathbf{s} \times \mathbf{d}), \mathbf{c}) \\
 &\stackrel{\text{(B.1b)}}{=} \frac{1}{2} \int_{\Omega} (\mathbf{s} \times \mathbf{d}) \cdot (\nabla \times \mathbf{c}) \, dx - \frac{1}{2} \int_{\partial\Omega} (\mathbf{s} \times \mathbf{d}) \cdot (\mathbf{c} \times \mathbf{n}) \, ds \\
 &\stackrel{\text{(B.1a)}}{=} \frac{1}{2} \int_{\Omega} \mathbf{d} \cdot [(\nabla \times \mathbf{c}) \times \mathbf{s}] \, dx - \frac{1}{2} \int_{\partial\Omega} \mathbf{d} \cdot [\mathbf{s} \times (\mathbf{c} \times \mathbf{n})] - (\mathbf{s} \times \mathbf{d}) \cdot (\mathbf{c} \times \mathbf{n}) \, ds \\
 &\stackrel{\text{(2.4)}}{=} \frac{1}{2} \int_{\Omega} \mathbf{d} \cdot [(\nabla \times \mathbf{c}) \times \mathbf{s}] \, dx \stackrel{\text{(4.4)}}{=} (\mathbf{d}, \overline{\mathcal{Z}}_b^* \mathbf{c}).
 \end{aligned}$$

The operator \mathcal{C}^* is identical to the one presented in [33].

6.2. Well posedness of the adjoint problem. In this section we prove the well-posedness of the adjoint problem §4.1 equation (4.5) using a saddle point type argument. To keep consistent with the standard setting of saddle point problems [27, 13], we use the notation $X := \mathbf{H}_0^1(\Omega) \times \mathbf{H}_\tau^1(\Omega)$ and $M := L^2(\Omega)$ so that $\mathcal{P} = X \times M$. We equip the space X with the graph norm

$$(6.5) \quad \|(\mathbf{v}, \mathbf{c})\|_X := (\|\mathbf{v}\|_1^2 + \|\mathbf{c}\|_1^2)^{1/2}.$$

We next define the bilinear form $a : X \times X \rightarrow \mathbb{R}$ by

$$\begin{aligned}
 (6.6) \quad a((\phi, \beta), (\mathbf{v}, \mathbf{c})) &= \frac{1}{\text{Re}} (\nabla \phi, \nabla \mathbf{v}) + (\overline{\mathcal{C}}^* \phi, \mathbf{v}) \\
 &+ \frac{\kappa}{\text{Re}_m} (\nabla \times \beta, \nabla \times \mathbf{c}) + \frac{\kappa}{\text{Re}_m} (\nabla \cdot \beta, \nabla \cdot \mathbf{c}) \\
 &- \kappa (\overline{\mathcal{Y}}^* \phi, \mathbf{c}) - \kappa (\overline{\mathcal{Z}}_u^* \beta, \mathbf{v}) - \kappa (\overline{\mathcal{Z}}_b^* \beta, \mathbf{c}),
 \end{aligned}$$

and the mixed form $b : X \times M \rightarrow \mathbb{R}$ by

$$(6.7) \quad b((\phi, \mathbf{c}), \pi) = (\pi, \nabla \cdot \phi).$$

The weak dual problem (4.5) is then equivalent to the following mixed problem: find $((\phi, \beta), \pi) \in X \times M$ such that

$$(6.8) \quad \begin{cases} a((\phi, \beta), (\mathbf{v}, \mathbf{c})) + b((\mathbf{v}, \mathbf{c}), \pi) = f(\mathbf{v}, \mathbf{c}), & \forall (\mathbf{v}, \mathbf{c}) \in X, \\ b((\phi, \beta), q) = -g(q), & \forall q \in M, \end{cases}$$

where $f(\mathbf{v}, \mathbf{c}) = (\psi_u, \mathbf{v}) + (\psi_b, \mathbf{c})$, $g(q) = (\psi_p, q)$ and $\Psi = [\psi_u, \psi_b, \psi_p]^T$ so that $(\Psi, V) = f(\mathbf{v}, \mathbf{c}) + g(q)$. According to the theory of saddle point systems, in order to show the existence and uniqueness of solutions to (6.8), it suffices to show:

- (i) The bilinear forms $a(\cdot, \cdot)$ and $b(\cdot, \cdot)$ are bounded on their respective domains.
- (ii) The form $a(\cdot, \cdot)$ is coercive on $X_0 := \{v \in X : b(v, q) = 0, \forall q \in M\}$.
- (iii) The form $b(\cdot, \cdot)$ satisfies the inf-sup condition: $\exists \beta > 0$ such that

$$(6.9) \quad \inf_{q \in M} \sup_{(\mathbf{v}, \mathbf{c}) \in X} \frac{b((\mathbf{v}, \mathbf{c}), q)}{\|(\mathbf{v}, \mathbf{c})\|_X \|q\|_M} \geq \beta.$$

We organize these parts in the following lemmas. We make frequent use of the inequalities in Appendix C in the proofs.

LEMMA 6.1. *The form $a(\cdot, \cdot)$ is bounded on X .*

Proof. Consider the splitting

$$(6.10) \quad a((\boldsymbol{\phi}, \boldsymbol{\beta}), (\mathbf{v}, \mathbf{c})) = a_0((\boldsymbol{\phi}, \boldsymbol{\beta}), (\mathbf{v}, \mathbf{c})) + a_1((\boldsymbol{\phi}, \boldsymbol{\beta}), (\mathbf{v}, \mathbf{c}))$$

where

$$\begin{aligned} a_0((\boldsymbol{\phi}, \boldsymbol{\beta}), (\mathbf{v}, \mathbf{c})) &= \frac{1}{\text{Re}} (\nabla \boldsymbol{\phi}, \nabla \mathbf{v}) + \frac{\kappa}{\text{Re}_m} (\nabla \times \boldsymbol{\beta}, \nabla \times \mathbf{c}) + \frac{\kappa}{\text{Re}_m} (\nabla \cdot \boldsymbol{\beta}, \nabla \cdot \mathbf{c}), \\ a_1((\boldsymbol{\phi}, \boldsymbol{\beta}), (\mathbf{v}, \mathbf{c})) &= (\overline{\mathcal{C}}^* \boldsymbol{\phi}, \mathbf{v}) - \kappa (\overline{\mathcal{Y}}^* \boldsymbol{\phi}, \mathbf{c}) - \kappa (\overline{\mathcal{Z}}_u^* \boldsymbol{\beta}, \mathbf{v}) - \kappa (\overline{\mathcal{Z}}_b^* \boldsymbol{\beta}, \mathbf{c}). \end{aligned}$$

Then it suffices to show that both $a_0(\cdot, \cdot)$ and $a_1(\cdot, \cdot)$ are bounded separately. The proof for the boundedness of a_0 is given in [42]. For a_1 observe that

$$(6.11) \quad \begin{aligned} |a_1((\boldsymbol{\phi}, \boldsymbol{\beta}), (\mathbf{v}, \mathbf{c}))| &\leq \int_{\Omega} |\overline{\mathcal{C}}^* \boldsymbol{\phi} \cdot \mathbf{v}| \, dx + \kappa \int_{\Omega} |\overline{\mathcal{Y}}^* \boldsymbol{\phi} \cdot \mathbf{c}| \, dx \\ &\quad + \kappa \int_{\Omega} |\overline{\mathcal{Z}}_u^* \boldsymbol{\beta} \cdot \mathbf{v}| \, dx + \kappa \int_{\Omega} |\overline{\mathcal{Z}}_b^* \boldsymbol{\beta} \cdot \mathbf{c}| \, dx. \end{aligned}$$

Now, for the first term on the right hand side of (6.11),

$$\begin{aligned} \int_{\Omega} |\overline{\mathcal{C}}^* \boldsymbol{\phi} \cdot \mathbf{v}| \, dx &= \frac{1}{2} \int_{\Omega} |[(\nabla \mathbf{s})^T \boldsymbol{\phi} - ((\mathbf{s} \cdot \nabla) \boldsymbol{\phi}) - (\nabla \cdot \mathbf{s}) \boldsymbol{\phi}] \cdot \mathbf{v}| \, dx \\ &= \frac{1}{2} \int_{\Omega} |\boldsymbol{\phi}^T (\nabla \mathbf{s}) \mathbf{v} - \mathbf{v}^T (\nabla \boldsymbol{\phi}) \mathbf{s} - (\nabla \cdot \mathbf{s}) (\boldsymbol{\phi} \cdot \mathbf{v})| \, dx \\ &\stackrel{\text{(C.5)}}{\leq} \frac{1}{2} [\|\boldsymbol{\phi}\|_{L^4} \|\mathbf{s}\|_1 \|\mathbf{v}\|_{L^4} + \|\boldsymbol{\phi}\|_1 \|\mathbf{s}\|_{L^4} \|\mathbf{v}\|_{L^4} + \|\nabla \cdot \mathbf{s}\| \|\boldsymbol{\phi} \cdot \mathbf{v}\|] \\ &\stackrel{\text{(B.2d)}}{\leq} \frac{1}{2} [\|\boldsymbol{\phi}\|_{L^4} \|\mathbf{s}\|_1 \|\mathbf{v}\|_{L^4} + \|\boldsymbol{\phi}\|_1 \|\mathbf{s}\|_{L^4} \|\mathbf{v}\|_{L^4} + \sqrt{3} \|\mathbf{s}\|_1 \|\boldsymbol{\phi}\|_{L^4} \|\mathbf{v}\|_{L^4}] \\ &\stackrel{\text{(C.1)}}{\leq} \frac{\gamma}{2} (\|\boldsymbol{\phi}\|_1 \|\mathbf{s}\|_1 \|\mathbf{v}\|_1 + \|\mathbf{s}\|_1 \|\boldsymbol{\phi}\|_1 \|\mathbf{v}\|_1 + \sqrt{3} \|\mathbf{s}\|_1 \|\boldsymbol{\phi}\|_1 \|\mathbf{v}\|_1) \\ &\leq \frac{3\sqrt{3}\gamma}{2} \|\mathbf{s}\|_1 \|\boldsymbol{\phi}\|_1 \|\mathbf{v}\|_1, \end{aligned}$$

where γ is the square of the embedding constant of $\mathbf{H}^1(\Omega)$ into $\mathbf{L}^4(\Omega)$, see (C.1). For the second term on the right hand side of (6.11),

$$\begin{aligned} \kappa (\overline{\mathcal{Y}}^* \boldsymbol{\phi} \cdot \mathbf{c}) &\leq \frac{\kappa}{2} \int_{\Omega} |\mathbf{c} \cdot [(\nabla \times \mathbf{t}) \times \boldsymbol{\phi}] + |\mathbf{c} \cdot [\nabla \times (\mathbf{t} \times \boldsymbol{\phi})]| \, dx \\ &\stackrel{\text{(B.1b)}}{=} \frac{\kappa}{2} \int_{\Omega} |\mathbf{c} \cdot ((\nabla \times \mathbf{t}) \times \boldsymbol{\phi})| + |(\nabla \times \mathbf{c}) \cdot (\mathbf{t} \times \boldsymbol{\phi})| \, dx \\ &\stackrel{\text{(B.1a)}}{=} \frac{\kappa}{2} \int_{\Omega} |(\nabla \times \mathbf{t}) \cdot (\mathbf{c} \times \boldsymbol{\phi})| + |(\nabla \times \mathbf{c}) \cdot (\mathbf{t} \times \boldsymbol{\phi})| \, dx \\ &\stackrel{\text{(B.2b)}}{\leq} \frac{\kappa}{2} (\|\nabla \times \mathbf{t}\|_{L^2} \|\mathbf{c}\|_{L^4} \|\boldsymbol{\phi}\|_{L^4} + \|\nabla \times \mathbf{c}\|_{L^2} \|\mathbf{t}\|_{L^4} \|\boldsymbol{\phi}\|_{L^4}) \\ &\stackrel{\text{(B.2c)}}{\leq} \frac{\kappa\sqrt{2}}{2} (\|\mathbf{c}\|_{L^4} \|\mathbf{t}\|_1 \|\boldsymbol{\phi}\|_{L^4} + \|\mathbf{c}\|_1 \|\mathbf{t}\|_{L^4} \|\boldsymbol{\phi}\|_{L^4}) \\ &\stackrel{\text{(C.1)}}{\leq} \kappa\gamma\sqrt{2} \|\mathbf{c}\|_1 \|\mathbf{t}\|_1 \|\boldsymbol{\phi}\|_1. \end{aligned}$$

For the third term on the right hand side of (6.11),

$$\begin{aligned} \kappa \left(\overline{\mathcal{Z}}_{\mathbf{u}}^* \boldsymbol{\beta}, \mathbf{v} \right) &\leq \frac{\kappa}{2} \int_{\Omega} |\mathbf{v} \cdot [\mathbf{t} \times (\nabla \times \boldsymbol{\beta})]| \, dx \stackrel{\text{(B.1b)}}{=} \frac{\kappa}{2} \int_{\Omega} |(\mathbf{v} \times \mathbf{t}) \cdot (\nabla \times \boldsymbol{\beta})| \, dx \\ &\stackrel{\text{(B.2c)}}{\leq} \frac{\kappa\sqrt{2}}{2} \|\mathbf{v}\|_{\mathbf{L}^4} \|\mathbf{t}\|_{\mathbf{L}^4} \|\boldsymbol{\beta}\|_1 \stackrel{\text{(C.1)}}{\leq} \frac{\kappa\gamma\sqrt{2}}{2} \|\mathbf{v}\|_1 \|\mathbf{t}\|_1 \|\boldsymbol{\beta}\|_1. \end{aligned}$$

The fourth term follows the same argument as the third term to yield the bound,

$$(6.12) \quad \kappa \left(\overline{\mathcal{Z}}_{\mathbf{b}}^* \boldsymbol{\beta}, \mathbf{c} \right) \leq \frac{\kappa\gamma\sqrt{2}}{2} \|\mathbf{c}\|_1 \|\mathbf{s}\|_1 \|\boldsymbol{\beta}\|_1.$$

Putting these bounds together, we conclude

$$\begin{aligned} a_1((\boldsymbol{\phi}, \boldsymbol{\beta}), (\mathbf{v}, \mathbf{c})) &\leq \gamma \left(\frac{3\sqrt{3}}{2} \|\mathbf{s}\|_1 \|\boldsymbol{\phi}\|_1 \|\mathbf{v}\|_1 + \kappa\sqrt{2} \|\mathbf{c}\|_1 \|\mathbf{t}\|_1 \|\boldsymbol{\phi}\|_1 \right. \\ &\quad \left. + \frac{\kappa\sqrt{2}}{2} \|\mathbf{v}\|_1 \|\mathbf{t}\|_1 \|\boldsymbol{\beta}\|_1 + \frac{\kappa\sqrt{2}}{2} \|\mathbf{c}\|_1 \|\mathbf{s}\|_1 \|\boldsymbol{\beta}\|_1 \right) \\ &\stackrel{\text{(C.2)}}{\leq} \gamma \left(\frac{3\sqrt{3}}{2} \|\mathbf{s}\|_1 \|\boldsymbol{\phi}\|_1 \|\mathbf{v}\|_1 + \frac{\kappa\sqrt{2}}{2} \|\mathbf{c}\|_1 \|\mathbf{s}\|_1 \|\boldsymbol{\beta}\|_1 \right. \\ (6.13) \quad &\quad \left. + \|\mathbf{t}\|_1 \kappa\sqrt{2} \|(\mathbf{v}, \mathbf{c})\|_X \|(\boldsymbol{\phi}, \boldsymbol{\beta})\|_X \right) \\ &\stackrel{\text{(C.2)}}{\leq} \gamma \left(\|\mathbf{s}\|_1 \max \left\{ \frac{3\sqrt{3}}{2}, \frac{\kappa\sqrt{2}}{2} \right\} \|(\mathbf{v}, \mathbf{c})\|_X \|(\boldsymbol{\phi}, \boldsymbol{\beta})\|_X \right. \\ &\quad \left. + \|\mathbf{t}\|_1 \|(\mathbf{v}, \mathbf{c})\|_X \|(\boldsymbol{\phi}, \boldsymbol{\beta})\|_X \right) \\ &\leq \alpha_b \|(\mathbf{v}, \mathbf{c})\|_X \|(\boldsymbol{\phi}, \boldsymbol{\beta})\|_X, \end{aligned}$$

where

$$\alpha_b = \max \left\{ \|\mathbf{s}\|_1 \max \left\{ \frac{3\sqrt{3}}{2}, \frac{\kappa\sqrt{2}}{2} \right\}, \|\mathbf{t}\|_1 \right\}.$$

□

Now we consider the coercivity of the bilinear form $a(\cdot, \cdot)$ on X .

LEMMA 6.2. *There exists a constant $\alpha_c > 0$ such that whenever*

$$(6.14) \quad \frac{k_1}{\text{Re}} - \gamma \left[\frac{3\sqrt{3}}{2} \|\mathbf{s}\|_1 + \frac{3\kappa\sqrt{2}}{4} \|\mathbf{t}\|_1 \right] > 0,$$

and

$$(6.15) \quad \frac{k_2\kappa}{\text{Re}_m^2} - \gamma \left[\frac{\kappa\sqrt{2}}{2} \|\mathbf{s}\|_1 + \frac{3\kappa\sqrt{2}}{4} \|\mathbf{t}\|_1 \right] > 0$$

then

$$(6.16) \quad a((\boldsymbol{\phi}, \boldsymbol{\beta}), (\boldsymbol{\phi}, \boldsymbol{\beta})) \geq \alpha_c \|(\boldsymbol{\phi}, \boldsymbol{\beta})\|_X^2, \quad \forall (\boldsymbol{\phi}, \boldsymbol{\beta}) \in X.$$

Proof. Using the splitting established in the previous lemma,

$$\begin{aligned}
(6.17) \quad & a((\boldsymbol{\phi}, \boldsymbol{\beta}), (\boldsymbol{\phi}, \boldsymbol{\beta})) \geq a_0((\boldsymbol{\phi}, \boldsymbol{\beta}), (\boldsymbol{\phi}, \boldsymbol{\beta})) - |a_1((\boldsymbol{\phi}, \boldsymbol{\beta}), (\boldsymbol{\phi}, \boldsymbol{\beta}))| \\
& = \frac{1}{\text{Re}} (\nabla \boldsymbol{\phi}, \nabla \boldsymbol{\phi}) + \frac{\kappa}{\text{Re}_m} (\nabla \times \boldsymbol{\beta}, \nabla \times \boldsymbol{\beta}) + \frac{\kappa}{\text{Re}_m} (\nabla \cdot \boldsymbol{\beta}, \nabla \cdot \boldsymbol{\beta}) \\
& - |a_1((\boldsymbol{\phi}, \boldsymbol{\beta}), (\boldsymbol{\phi}, \boldsymbol{\beta}))| \\
& \geq \frac{k_1}{\text{Re}} \|\boldsymbol{\phi}\|_1^2 + \frac{k_2 \kappa}{\text{Re}_m^2} \|\boldsymbol{\beta}\|_1^2 - |a_1((\boldsymbol{\phi}, \boldsymbol{\beta}), (\boldsymbol{\phi}, \boldsymbol{\beta}))|
\end{aligned}$$

where k_1 comes from the Poincaré type inequality (C.3), and k_2 is defined though

$$(6.18) \quad \|\nabla \times \mathbf{v}\|_0^2 + \|\nabla \cdot \mathbf{v}\|_0^2 \geq k_2 \|\mathbf{v}\|_1^2, \quad \forall \mathbf{v} \in \mathbf{H}_\tau^1(\Omega),$$

which is valid under the restrictions we have imposed on the domain Ω and the continuous embedding of $\mathbf{H}_\tau^1(\Omega) \hookrightarrow \mathbf{H}^1(\Omega)$ [40, 42]. Picking up from (6.17) and using (C.4) we conclude that,

$$\begin{aligned}
& a((\boldsymbol{\phi}, \boldsymbol{\beta}), (\boldsymbol{\phi}, \boldsymbol{\beta})) \geq \frac{k_1}{\text{Re}} \|\boldsymbol{\phi}\|_1^2 + \frac{k_2 \kappa}{\text{Re}_m^2} \|\boldsymbol{\beta}\|_1^2 - |a_1((\boldsymbol{\phi}, \boldsymbol{\beta}), (\boldsymbol{\phi}, \boldsymbol{\beta}))| \\
& \stackrel{(6.13)}{\geq} \left(\frac{k_1}{\text{Re}} - \frac{\gamma 3\sqrt{3}}{2} \|\mathbf{s}\|_1 \right) \|\boldsymbol{\phi}\|_1^2 + \left(\frac{k_2 \kappa}{\text{Re}_m^2} - \frac{\gamma \kappa \sqrt{2}}{2} \|\mathbf{s}\|_1 \right) \|\boldsymbol{\beta}\|_1^2 \\
& - \frac{\gamma 3\kappa \sqrt{2}}{2} \|\boldsymbol{\phi}\|_1 \|\mathbf{t}\|_1 \|\boldsymbol{\beta}\|_1 \\
& \stackrel{(C.4)}{\geq} \left(\frac{k_1}{\text{Re}} - \frac{\gamma 3\sqrt{3}}{2} \|\mathbf{s}\|_1 \right) \|\boldsymbol{\phi}\|_1^2 + \left(\frac{k_2 \kappa}{\text{Re}_m^2} - \frac{\gamma \kappa \sqrt{2}}{2} \|\mathbf{s}\|_1 \right) \|\boldsymbol{\beta}\|_1^2 \\
& - \frac{\gamma 3\kappa \sqrt{2}}{4} \|\mathbf{t}\|_1 (\|\boldsymbol{\beta}\|_1^2 + \|\boldsymbol{\phi}\|_1^2) \\
& = \left(\frac{k_1}{\text{Re}} - \gamma \left[\frac{3\sqrt{3}}{2} \|\mathbf{s}\|_1 + \frac{3\kappa \sqrt{2}}{4} \|\mathbf{t}\|_1 \right] \right) \|\boldsymbol{\phi}\|_1^2 \\
& + \left(\frac{k_2 \kappa}{\text{Re}_m^2} - \gamma \left[\frac{\kappa \sqrt{2}}{2} \|\mathbf{s}\|_1 + \frac{3\kappa \sqrt{2}}{4} \|\mathbf{t}\|_1 \right] \right) \|\boldsymbol{\beta}\|_1^2.
\end{aligned}$$

Thus, taking

$$(6.19) \quad \alpha_c = \min \left\{ \frac{k_1}{\text{Re}} - \gamma \left[\frac{3\sqrt{3}}{2} \|\mathbf{s}\|_1 + \frac{3\kappa \sqrt{2}}{4} \|\mathbf{t}\|_1 \right], \right. \\
\left. \frac{k_2 \kappa}{\text{Re}_m^2} - \gamma \left[\frac{\kappa \sqrt{2}}{2} \|\mathbf{s}\|_1 + \frac{3\kappa \sqrt{2}}{4} \|\mathbf{t}\|_1 \right] \right\},$$

concludes the lemma. \square

REMARK 2. We note that the quantities assumed to be positive in (6.14) and (6.15), depend on the computed and true solutions through $\|\mathbf{s}\|$ and $\|\mathbf{t}\|$, which should both be bounded for “small data” as described precisely in Theorem 4.7 of [42]. The two quantities in (6.14) and (6.15) also depend on the fluid and magnetic Reynolds numbers (Re and Re_m respectively). In particular, for small to moderate

Re and Re_m these inequalities might very well be satisfied, which is the case for dissipative MHD. However, the larger are Re and Re_m (and in particular for the limit as $\text{Re}, \text{Re}_m \rightarrow \infty$, that is in the case of ideal MHD), the smaller the positive terms of (6.14) and (6.15), and thus coercivity cannot be proven by this method. We conclude this method might therefore need to be adapted for high Re or Re_m flows to guarantee coercivity.

Now we are prepared to prove the main result.

THEOREM 6.3. *Under the conditions of Lemma 6.2 there exists a unique solution to the dual problem (4.5).*

Proof. The boundedness and inf-sup condition for $b(\cdot, \cdot)$ are standard see e.g. [13]. The boundedness of $a(\cdot, \cdot)$ follows from Lemma 6.1, and Lemma 6.2 proves $a(\cdot, \cdot)$ is coercive on X so in particular on X_0 . \square

7. Conclusions. We have presented an adjoint-based *a posteriori* analysis of adjoint for an exact penalty formulation of incompressible resistive MHD. This included the derivation of the adjoint error estimate, and a development that characterized the separate contributions of error from the momentum, continuity and magnetic field equations. The numerical examples illustrated both the accuracy as well as the usefulness of the error estimate for the the assessment of the respective sources of the error from the different physics components. The example QoIs included two differing physically meaningful quantities, the averaged velocity-related to the flow rate, and the induced magnetic field strength.

The novel aspects of this work include defining an adjoint problem for an overdetermined system, namely the stationary MHD equations. In particular, the standard definition of an adjoint operator does not suffice and we must define the adjoint directly for the weak problem. Moreover, we prove the well-posedness of the adjoint problem. The error estimates derived in this article are also amenable for using in adaptive refinement algorithms e.g. see [5, 14, 6, 20, 36, 16].

Appendix A. Standard function spaces. We denote by $L^2(\Omega)$ the set of all square Lebesgue integrable functions on $\Omega \subset \mathbb{R}^d$ with associated inner product (\cdot, \cdot) and norm $\|\cdot\|$. This extends naturally to vector valued functions, denoted by $\mathbf{L}^2(\Omega)$, where the inner product is given by,

$$(\mathbf{u}, \mathbf{v}) = \sum_{i=1}^d (u_i, v_i).$$

The Sobolev norm for $p = 2$ is,

$$\|v\|_m := \left(\sum_{|\alpha|=0}^m \|D^\alpha v\|^2 \right)^{1/2}.$$

where $\alpha = (\alpha_1, \dots, \alpha_m)$ is a multi-index of length m and

$$D^\alpha v := \partial_{x_1}^{\alpha_1} \dots \partial_{x_m}^{\alpha_m} v,$$

where the partial derivatives are taken in the weak sense. Thus, the Hilbert spaces H^m for $m = 0, 1, 2, \dots$ is simply be defined as functions with bounded m -norm,

$$H^m(\Omega) := \{v : \|v\|_m < \infty\}.$$

The space $H^0(\Omega)$ is identified with $L^2(\Omega)$. For vector valued functions, the Hilbert space \mathbf{H}^m is defined as,

$$\mathbf{H}^m(\Omega) := \{\mathbf{v} : v_i \in H^m(\Omega), i = 1, \dots, d\},$$

with associated norm

$$\|\mathbf{v}\|_m = \left(\sum_{i=1}^d \|v_i\|_m^2 \right)^{1/2}.$$

Appendix B. Vector identities and inequalities. We use the following vector identities,

$$(B.1a) \quad \mathbf{A} \cdot (\mathbf{B} \times \mathbf{C}) = \mathbf{B} \cdot (\mathbf{C} \times \mathbf{A}) = \mathbf{C} \cdot (\mathbf{A} \times \mathbf{B}),$$

$$(B.1b) \quad \int_{\Omega} \mathbf{A} \cdot (\nabla \times \mathbf{B}) \, dx = \int_{\Omega} \mathbf{B} \cdot (\nabla \times \mathbf{A}) \, dx - \int_{\partial\Omega} \mathbf{B} \cdot (\mathbf{A} \times \mathbf{n}) \, ds.$$

We also make use of the following inequalities for $\mathbf{u}, \mathbf{v} \in \mathbf{H}^1(\Omega)$,

$$(B.2a) \quad |\mathbf{u} \cdot \mathbf{v}| \leq \|\mathbf{u}\|_{\mathbb{R}^d} \|\mathbf{v}\|_{\mathbb{R}^d},$$

$$(B.2b) \quad \|\mathbf{u} \times \mathbf{v}\|_{\mathbb{R}^d} \leq \|\mathbf{u}\|_{\mathbb{R}^d} \|\mathbf{v}\|_{\mathbb{R}^d},$$

$$(B.2c) \quad \|\nabla \times \mathbf{u}\|_{\mathbb{R}^d} \leq \sqrt{2} \|\nabla \mathbf{u}\|_{\mathbb{R}^{d \times d}},$$

$$(B.2d) \quad \|\nabla \cdot \mathbf{u}\| \leq \sqrt{3} \|\nabla \mathbf{u}\|_{\mathbb{R}^{d \times d}}$$

$$(B.2e) \quad \|\mathbf{A}\mathbf{v}\|_{\mathbb{R}^d} \leq \|\mathbf{A}\|_{\mathbb{R}^{d \times d}} \|\mathbf{v}\|_{\mathbb{R}^d},$$

and finally the equality

$$(B.3) \quad \|\nabla \mathbf{v}^T\|_{\mathbb{R}^{d \times d}} = \|\nabla \mathbf{v}\|_{\mathbb{R}^{d \times d}},$$

Appendix C. Useful inequalities from analysis.

1. The space $\mathbf{H}^1(\Omega)$ embeds continuously in $\mathbf{L}^4(\Omega)$ with constant $\sqrt{\gamma}$. That is, $\mathbf{H}^1(\Omega) \hookrightarrow \mathbf{L}^4(\Omega)$ such that,

$$(C.1) \quad \|\mathbf{v}\|_{\mathbf{L}^4} \leq \sqrt{\gamma} \|\mathbf{v}\|_{\mathbf{H}^1}.$$

2. The Cauchy-Schwarz inequality for $[a, b], [c, d] \in \mathbb{R}^2$,

$$(C.2) \quad ac + bd = [a, b] [c, d]^T \leq \sqrt{a^2 + c^2} \sqrt{b^2 + d^2},$$

3. The following inequality follows from the Poincaré inequality,

$$(C.3) \quad \|\nabla \mathbf{v}\|_0^2 \geq k_1 \|\mathbf{v}\|_1^2, \quad \forall \mathbf{v} \in \mathbf{H}_0^1(\Omega).$$

4. For $x, y \in \mathbb{R}$,

$$(C.4) \quad -xy \geq -\frac{1}{2}(x^2 + y^2),$$

We also need the following propositions,

PROPOSITION 1. *Let $\mathbf{u}, \mathbf{v}, \mathbf{w} \in \mathbf{H}^1(\Omega)$. Then there holds*

$$(C.5) \quad \int_{\Omega} \mathbf{u}^T (\nabla \mathbf{v}) \mathbf{w} \, dx \leq \|\mathbf{u}\|_{\mathbf{L}^4} \|\mathbf{w}\|_{\mathbf{L}^4} \|\mathbf{v}\|_1.$$

Proof. We will work with the integrand first. To this end, we have that

$$\begin{aligned} \mathbf{u}^T(\nabla \mathbf{v})\mathbf{w} &= \sum_{i=1}^d u_i \mathbf{w}^T \nabla v_i \leq \sum_{i=1}^d |u_i| \|\mathbf{w}\|_{\mathbb{R}^d} \|\nabla v_i\|_{\mathbb{R}^d} = \|\mathbf{w}\|_{\mathbb{R}^d} \sum_{i=1}^d |u_i| \|\nabla v_i\|_{\mathbb{R}^d} \\ &\leq \|\mathbf{w}\|_{\mathbb{R}^d} \left(\sum_{i=1}^d |u_i|^2 \right)^{1/2} \left(\sum_{i=1}^d \|\nabla v_i\|_{\mathbb{R}^d}^2 \right)^{1/2} = \|\mathbf{w}\|_{\mathbb{R}^d} \|\mathbf{u}\|_{\mathbb{R}^d} \|\nabla \mathbf{v}\|_{\mathbb{R}^{d \times d}}. \end{aligned}$$

Now we integrate,

$$\begin{aligned} &\int_{\Omega} |\mathbf{w}|_{\mathbb{R}^d} \|\mathbf{u}\|_{\mathbb{R}^d} \|\nabla \mathbf{v}\|_{\mathbb{R}^{d \times d}} \, dx \\ &\leq \left(\int_{\Omega} \|\mathbf{u}\|_{\mathbb{R}^d}^2 \|\mathbf{w}\|_{\mathbb{R}^d}^2 \, dx \right)^{1/2} \left(\int_{\Omega} \|\nabla \mathbf{v}\|_{\mathbb{R}^{d \times d}}^2 \, dx \right)^{1/2} \\ &\leq \left(\int_{\Omega} \|\mathbf{u}\|_{\mathbb{R}^d}^4 \, dx \right)^{1/4} \left(\int_{\Omega} \|\mathbf{w}\|_{\mathbb{R}^d}^4 \, dx \right)^{1/4} \left(\int_{\Omega} \|\nabla \mathbf{v}\|_{\mathbb{R}^{d \times d}}^2 \, dx \right)^{1/2} \\ &= \|\mathbf{u}\|_{L^4} \|\mathbf{w}\|_{L^4} \|\mathbf{v}\|_1 \leq \|\mathbf{u}\|_{L^4} \|\mathbf{w}\|_{L^4} \|\mathbf{v}\|_1. \quad \square \end{aligned}$$

REFERENCES

- [1] J. H. ADLER, M. BREZINA, T. A. MANTEUFFEL, S. F. MCCORMICK, J. W. RUGE, AND L. TANG, *Island coalescence using parallel first-order system least squares on incompressible resistive magnetohydrodynamics*, SIAM Journal on Scientific Computing, 35 (2013), pp. S171–S191.
- [2] J. H. ADLER, Y. HE, X. HU, AND S. P. MACLACHLAN, *Vector-potential finite-element formulations for two-dimensional resistive magnetohydrodynamics*, Computers & Mathematics with Applications, 77 (2019), pp. 476–493.
- [3] J. H. ADLER, T. A. MANTEUFFEL, S. F. MCCORMICK, AND J. W. RUGE, *First-order system least squares for incompressible resistive magnetohydrodynamics*, SIAM Journal on Scientific Computing, 32 (2010), pp. 229–248.
- [4] J. H. ADLER, T. A. MANTEUFFEL, S. F. MCCORMICK, J. W. RUGE, AND G. D. SANDERS, *Nested iteration and first-order system least squares for incompressible, resistive magnetohydrodynamics*, SIAM Journal on Scientific Computing, 32 (2010), pp. 1506–1526.
- [5] M. AINSWORTH AND T. ODEN, *A posteriori error estimation in finite element analysis*, John Wiley-Teubner, 2000.
- [6] B. AKSOYLU, S. D. BOND, E. C. CYR, AND M. HOLST, *Goal-oriented adaptivity and multilevel preconditioning for the Poisson-Boltzmann equation*, Journal of Scientific Computing, 52 (2011), pp. 202–225.
- [7] M. S. ALNÆS, J. BLECHTA, J. HAKE, A. JOHANSSON, B. KEHLET, A. LOGG, C. RICHARDSON, J. RING, M. E. ROGNES, AND G. N. WELLS, *The fenics project version 1.5*, Archive of Numerical Software, 3 (2015).
- [8] W. BANGERTH AND R. RANNACHER, *Adaptive Finite Element Methods for Differential Equations*, Birkhauser Verlag, 2003.
- [9] T. J. BARTH, *A posteriori Error Estimation and Mesh Adaptivity for Finite Volume and Finite Element Methods*, vol. 41 of Lecture Notes in Computational Science and Engineering, Springer, New York, 2004.
- [10] R. BECKER AND R. RANNACHER, *An optimal control approach to a posteriori error estimation in finite element methods: Acta numerica*, Jan 2003.
- [11] P. BOCHEV AND A. ROBINSON, *Matching algorithms with physics: exact sequences of finite element spaces*, Collected Lectures on the Preservation of Stability Under Discretization, edited by D. Estep and S. Tavener, SIAM, Philadelphia, (2001).
- [12] D. BOFFI, F. BREZZI, M. FORTIN, ET AL., *Mixed finite element methods and applications*, vol. 44, Springer, 2013.
- [13] S. C. BRENNER AND L. R. SCOTT, *The mathematical theory of finite element methods*, Springer, 2011.

- [14] V. CAREY, D. ESTEP, A. JOHANSSON, M. LARSON, AND S. TAVENER, *Blockwise adaptivity for time dependent problems based on coarse scale adjoint solutions*, SIAM Journal on Scientific Computing, 32 (2010), pp. 2121–2145.
- [15] V. CAREY, D. ESTEP, AND S. TAVENER, *A posteriori analysis and adaptive error control for multiscale operator decomposition solution of elliptic systems I: One way coupled systems*, SIAM Journal on Numerical Analysis, 47 (2009), pp. 740–761.
- [16] J. H. CHAUDHRY, *A posteriori analysis and efficient refinement strategies for the poisson-boltzmann equation*, SIAM Journal on Scientific Computing, 40 (2018), pp. A2519–A2542.
- [17] J. H. CHAUDHRY, N. BURCH, AND D. ESTEP, *Efficient distribution estimation and uncertainty quantification for elliptic problems on domains with stochastic boundaries*, SIAM/ASA Journal on Uncertainty Quantification, 6 (2018), pp. 1127–1150.
- [18] J. H. CHAUDHRY, J. COLLINS, AND J. N. SHADID, *A posteriori error estimation for multi-stage runge-kutta IMEX schemes*, Applied Numerical Mathematics, 117 (2017), pp. 36–49.
- [19] J. H. CHAUDHRY, D. ESTEP, V. GINTING, J. N. SHADID, AND S. TAVENER, *A posteriori error analysis of imex multi-step time integration methods for advection-diffusion-reaction equations*, Computer Methods in Applied Mechanics and Engineering, 285 (2015), pp. 730–751.
- [20] J. H. CHAUDHRY, D. ESTEP, S. TAVENER, V. CAREY, AND J. SANDELIN, *A posteriori error analysis of two-stage computation methods with application to efficient discretization and the Parareal algorithm*, SIAM Journal on Numerical Analysis, 54 (2016), pp. 2974–3002.
- [21] J. H. CHAUDHRY, J. N. SHADID, AND T. WILDEY, *A posteriori analysis of an IMEX entropy-viscosity formulation for hyperbolic conservation laws with dissipation*, Applied Numerical Mathematics, 135 (2019), pp. 129–142.
- [22] J. M. CONNORS, J. W. BANKS, J. A. HITTINGER, AND C. S. WOODWARD, *Quantification of errors for operator-split advection-diffusion calculations*, Computer Methods in Applied Mechanics and Engineering, 272 (2014), pp. 181–197.
- [23] E. C. CYR, J. SHADID, AND T. WILDEY, *Approaches for adjoint-based a posteriori analysis of stabilized finite element methods*, SIAM Journal on Scientific Computing, 36 (2014), pp. A766–A791.
- [24] A. DEDNER, F. KEMM, D. KRONER, C.-D. MUNZ, T. SCHNITZER, AND M. WESENBERG, *Hyperbolic divergence cleaning for the MHD equations*, Journal of Computational Physics, 175 (2002), pp. 645–673.
- [25] K. ERIKSSON, D. ESTEP, P. HANSBO, AND C. JOHNSON, *Introduction to adaptive methods for differential equations*, Acta Numerica, 4 (1995), pp. 105–158.
- [26] K. ERIKSSON, D. ESTEP, P. HANSBO, AND C. JOHNSON, *Computational Differential Equations*, Cambridge University Press, Cambridge, 1996.
- [27] A. ERN AND J.-L. GUERMOND, *Theory and practice of finite elements*, Springer, 2011.
- [28] D. ESTEP, *A posteriori error bounds and global error control for approximation of ordinary differential equations*, SIAM Journal on Numerical Analysis, 32 (1995), pp. 1–48.
- [29] D. ESTEP, V. GINTING, D. ROPP, J. N. SHADID, AND S. TAVENER, *An a posteriori-a priori analysis of multiscale operator splitting*, SIAM Journal on Numerical Analysis, 46 (2008), pp. 1116–1146.
- [30] D. ESTEP, A. MÅLQVIST, AND S. TAVENER, *Nonparametric density estimation for randomly perturbed elliptic problems I: Computational methods, a posteriori analysis, and adaptive error control*, SIAM J. Sci. Comput., 31 (2009), pp. 2935–2959.
- [31] D. ESTEP, A. MÅLQVIST, AND S. TAVENER, *Nonparametric density estimation for randomly perturbed elliptic problems I: Computational methods, a posteriori analysis, and adaptive error control*, SIAM Journal on Scientific Computing, 31 (2009), pp. 2935–2959.
- [32] D. ESTEP, A. MÅLQVIST, AND S. TAVENER, *Nonparametric density estimation for randomly perturbed elliptic problems II: Applications and adaptive modeling*, International Journal for Numerical Methods in Engineering, 80 (2009).
- [33] D. ESTEP, S. TAVENER, AND T. WILDEY, *A posteriori error estimation and adaptive mesh refinement for a multiscale operator decomposition approach to fluid-solid heat transfer*, Journal of Computational Physics, 229 (2010), pp. 4143–4158.
- [34] D. J. ESTEP, M. G. LARSON, R. D. WILLIAMS, AND A. M. SOCIETY, *Estimating the error of numerical solutions of systems of reaction-diffusion equations*, American Mathematical Society, 2000.
- [35] C. R. EVANS AND J. F. HAWLEY, *Simulation of magnetohydrodynamic flows: A constrained transport model*, Astrophysical Journal, 332 (1988), p. 659.
- [36] K. J. FIDKOWSKI AND D. L. DARMOFAL, *Review of output-based error estimation and mesh adaptation in computational fluid dynamics*, AIAA Journal, 49 (2011), pp. 673–694.
- [37] J.-F. GERBEAU, *A stabilized finite element method for the incompressible magnetohydrody-*

- namic equations*, *Numerische Mathematik*, 87 (2000), pp. 83–111.
- [38] J.-F. GERBEAU, C. L. BRIS, AND T. LELIÈVRE, *Mathematical Methods for the Magnetohydrodynamics of Liquid Metals*, Oxford University Press, Aug. 2006.
- [39] M. B. GILES AND E. SÜLI, *Adjoint methods for PDEs: a posteriori error analysis and postprocessing by duality*, *Acta Numerica* 2002, (2002), p. 145–236.
- [40] V. GIRAULT AND P.-A. RAVIART, *Finite Element Methods for Navier-Stokes Equations*, Springer Berlin Heidelberg, 1986.
- [41] J. P. H. GOEDBLOED, S. POEDTS, A. MILLS, AND S. ROMAINE, *Principles of Magnetohydrodynamics: With Applications to Laboratory and Astrophysical Plasmas*, Cambridge University Press, 2003.
- [42] M. D. GUNZBURGER, A. J. MEIR, AND J. S. PETERSON, *On the existence, uniqueness, and finite element approximation of solutions of the equations of stationary, incompressible magnetohydrodynamics*, *Mathematics of Computation*, 56 (1991), pp. 523–523.
- [43] M. HAMOUDA, R. TEMAM, AND L. ZHANG, *Modeling the lid driven flow: Theory and computation*, *International Journal of Numerical Analysis and Modeling*, 14 (2017), pp. 313–341.
- [44] P.-W. HSIEH AND S.-Y. YANG, *A bubble-stabilized least-squares finite element method for steady MHD duct flow problems at high hartmann numbers*, *Journal of Computational Physics*, 228 (2009), pp. 8301–8320.
- [45] J. M. HYMAN AND M. SHASHKOV, *Adjoint operators for the natural discretizations of the divergence, gradient and curl on logically rectangular grids*, *Applied Numerical Mathematics*, 25 (1997), pp. 413–442.
- [46] D. KUZMIN AND N. KLYUSHNEV, *Limiting and divergence cleaning for continuous finite element discretizations of the MHD equations*, *Journal of Computational Physics*, 407 (2020), p. 109230.
- [47] M. W. LEE, E. H. DOWELL, AND M. J. BALAJEWICZ, *A study of the regularized lid-driven cavity's progression to chaos*, Nov 2018.
- [48] P. LIN, J. SHADID, J. HU, R. PAWLOWSKI, AND E. CYR, *Performance of fully-coupled algebraic multigrid preconditioners for large-scale VMS resistive MHD*, *Journal of Computational and Applied Mathematics*, 344 (2018), pp. 782–793.
- [49] P. T. LIN, J. N. SHADID, AND P. H. TSUJI, *On the performance of krylov smoothing for fully coupled AMG preconditioners for VMS resistive MHD*, *International Journal for Numerical Methods in Engineering*, 120 (2019), pp. 1297–1309.
- [50] A. LOGG, K.-A. MARDAL, G. N. WELLS, ET AL., *Automated Solution of Differential Equations by the Finite Element Method*, Springer, 2012.
- [51] A. LOGG, G. N. WELLS, AND J. HAKE, *DOLFIN: a C++/Python Finite Element Library*, Springer, 2012.
- [52] G. I. MARCHUK, *Adjoint Equations and Analysis of Complex Systems*, Springer Nature, 1995.
- [53] G. I. MARCHUK, V. I. AGOSHKOV, AND V. P. SHUTYAEV, *Adjoint equations and perturbation algorithms in nonlinear problems*, CRC Press, 1996.
- [54] MARTIN AND M. DAUGE, *Weighted regularization of maxwell equations in polyhedral domains*, Dec 2002.
- [55] S. MILLER, E. CYR, J. SHADID, R. KRAMER, E. PHILLIPS, S. CONDE, AND R. PAWLOWSKI, *IMEX and exact sequence discretization of the multi-fluid plasma model*, *Journal of Computational Physics*, 397 (2019), p. 108806.
- [56] J. C. NEDELEC, *Mixed finite elements in \mathbb{R}^3* , *Numerische Mathematik*, 35 (1980), p. 315–341.
- [57] E. G. PHILLIPS, H. C. ELMAN, E. C. CYR, J. N. SHADID, AND R. P. PAWLOWSKI, *A block preconditioner for an exact penalty formulation for stationary MHD*, *SIAM Journal on Scientific Computing*, 36 (2014).
- [58] D. SCHOTZAU, *Mixed finite element methods for stationary incompressible magnetohydrodynamics*, *Numerische Mathematik*, 96 (2004), p. 771–800.
- [59] J. SHADID, R. PAWLOWSKI, J. BANKS, L. CHACÓN, P. LIN, AND R. TUMINARO, *Towards a scalable fully-implicit fully-coupled resistive MHD formulation with stabilized FE methods*, *Journal of Computational Physics*, 229 (2010), pp. 7649–7671.
- [60] S. SIVASANKARAN, A. MALLESWARAN, J. LEE, AND P. SUNDAR, *Hydro-magnetic combined convection in a lid-driven cavity with sinusoidal boundary conditions on both sidewalls*, *International Journal of Heat and Mass Transfer*, 54 (2011), pp. 512–525.
- [61] R. TEMAM, *Navier–Stokes Equations: Theory and Numerical Analysis*, American Mathematical Society, Apr. 2001.
- [62] J. P. TRELLES AND S. M. MODIRKHAZENI, *Variational multiscale method for nonequilibrium plasma flows.*, *Computer Methods in Applied Mechanics and Engineering*, 282 (2014), pp. 87 – 131.
- [63] M. ÜLRICH AND B. LEO, *Magnetofluidynamics in Channels and Containers*, Springer, 2010.